RESEARCH ARTICLE

Review on Unmanned Aerial Vehicle Assisted Sensor Node Localization in Wireless Networks: Soft Computing Approaches

VISALAKSHI ANNEPU[1], **DEEPIKA RANI SONA**[1], **CHINTHAGINJALA V. RAVIKUMAR**[1],
KALAPRAVEEN BAGADI[1], **MOHAMMAD ALIBAKHSHIKENARI**[2], (Member, IEEE),
AYMAN A. ALTHUWAYB[3], (Member, IEEE), **BADER ALALI**[3,4],
BAL S. VIRDEE[5], (Senior Member, IEEE), **GIOVANNI PAU**[6], (Member, IEEE),
IYAD DAYOUB[7,8], (Senior Member, IEEE), **CHAN HWANG SEE**[9], (Senior Member, IEEE),
AND FRANCISCO FALCONE[10,11], (Senior Member, IEEE)

[1]School of Electronics Engineering, Vellore Institute of Technology, Vellore 632014, India
[2]Department of Signal Theory and Communications, Universidad Carlos III de Madrid, Leganés, 28911 Madrid, Spain
[3]Department of Electrical Engineering, College of Engineering, Jouf University, Sakaka, Aljouf 72388, Saudi Arabia
[4]Center for Wireless Communications, Institute of Electronic, Communications and Information Technology, Queen's University Belfast, BT3 9DT Belfast, U.K.
[5]Center for Communications Technology, London Metropolitan University, N7 8DB London, U.K.
[6]Faculty of Engineering and Architecture, Kore University of Enna, 94100 Enna, Italy
[7]Université Polytechnique Hauts-de-France, Institut d'Électronique de Microélectronique et de Nanotechnologie (IEMN) CNRS UMR 8520, ISEN, Centrale Lille, University of Lille, 59313 Valenciennes, France
[8]INSA Hauts-de-France, 59313 Valenciennes, France
[9]School of Engineering and the Built Environment, Edinburgh Napier University, EH10 5DT Edinburgh, U.K.
[10]Department of Electric, Electronic, Communication Engineering, and Institute of Smart Cities, Public University of Navarre, 31006 Pamplona, Spain
[11]Tecnologico de Monterrey, School of Engineering and Sciences, Monterrey 64849, Mexico

Corresponding authors: Kalapraveen Bagadi (kpbagadi@gmail.com), Mohammad Alibakhshikenari
(mohammad.alibakhshikenari@uc3m.es), Giovanni Pau (giovanni.pau@unikore.it), and Francisco Falcone
(francisco.falcone@unavarra.es)

ABSTRACT Node positioning or localization is a critical requisite for numerous position-based applications of wireless sensor network (WSN). Localization using the unmanned aerial vehicle (UAV) is preferred over localization using fixed terrestrial anchor node (FTAN) because of low implementation complexity and high accuracy. The conventional multilateration technique estimates the position of the unknown node (UN) based on the distance from the anchor node (AN) to UN that is obtained from the received signal strength (RSS) measurement. However, distortions in the propagation medium may yield incorrect distance measurement and as a result, the accuracy of RSS-multilateration is limited. Though the optimization based localization schemes are considered to be a better alternative, the performance of these schemes is not satisfactory if the distortions are non-linear. In such situations, the neural network (NN) architecture such as extreme learning machine (ELM) can be a better choice as it is a highly non-linear classifier. The ELM is even superior over its counterpart NN classifiers like multilayer perceptron (MLP) and radial basis function (RBF) due to its fast and strong learning ability. Thus, this paper provides a comparative review of various soft computing based localization techniques using both FTAN and aerial ANs for better acceptability.

INDEX TERMS Extreme learning machine, localization, unmanned aerial vehicles, wireless sensor networks.

The associate editor coordinating the review of this manuscript and
approving it for publication was Stefano Scanzio.

I. INTRODUCTION

Recent advancements in communication systems have permitted the use of tiny, low-power, low-cost and multi-functional sensors [1], [2]. Many such tiny sensors are connected together to make a WSN that is used for several applications. Some of the applications of WSN include environment monitoring [3], traffic control [4], military surveillance [5], health observation [6], [7], industrial sensing [8] and so on. These sensors can be deployed in large numbers in the area of interest, to monitor and/or control the environment, homes or buildings. The sensors are connected together via wireless links and communicate among each other within their communication range. These low power sensors are capable of measuring environmental phenomena, processing information and communicating this information to other sensors wirelessly. These sensors are capable of measuring or detecting physical quantities such as pressure, temperature, or humidity and communicate this information to short distances [9]. The sensed data is useful only if we have priori information on the location of the wireless sensor nodes in the network. The procedure for acquiring location of nodes is usually called localization or positioning. The sensors in the given field should be placed strategically to achieve high localization accuracy [10].

A localization technique commonly used in outdoor environments is global positioning system (GPS) [11]. However, the deployment cost and energy utility will be higher for high dense sensor networks. In addition to that, GPS also needs line-of-sight (LoS) communication between the satellite and the UN. Thus, the usage of the GPS module is not recommended in every sensor node [12]. Instead, some position aware sensors can be nominated as ANs or beacon nodes (BNs) and by the use of these ANs, coordinates of remaining UNs can be obtained. This approach is called localization or positioning. Such localization is able to minimize energy consumption and deployment cost, effectively. Localization can be either FTAN assisted localization or mobile aerial anchor node (MAAN) assisted localization. In the MAAN system, the ANs are deployed in low altitude UAVs, whereas in the FTAN system, the ANs are deployed on the ground itself. The MAAN offers better localization accuracy over FTAN because the information from ANs is passed to UN through air to ground (AG) channel link, where nearly a clear LoS may occur [13], [14]. The accuracy of the FTAN system is limited because the information is passed from ANs to UNs through an erratic ground to ground (GG) channel, which imposes severe distortions.

Recent developments of software and hardware technologies and broad availability of UAVs permitted us to use them in diverse applications such as disaster management [15], [16], surveillance [17], agriculture fields [18] and many more. Due to aerial advantage the UAV based communication is also energy efficient [19]. Such unique capabilities of UAVs are also permitted them to use in 5G wireless networks [20], [21]. One more prime application of UAV is the node localization in WSN [22]. The node localization can be performed by either single UAV [23], [24] or multiple UAVs [25], [26]. Multiple UAVs are useful for fast localization and single UAV is useful for minimum implementation cost as it requires only one GPS module. During the past few decades, significant research contributions have been paid to develop various localization techniques using ground ANs. However, research contribution in localization using aerial ANs still requires substantial attention. Firstly, in ground AN-based localization, one of the popular classifications of various localization schemes is made according to the mobility of ANs and UNs [27], [28]. Hence, the localization techniques are classified into four categories namely, static ANs and static UNs [29], [30], [31], static ANs and mobile UNs [32], mobile ANs and static UNs [33], [34], [35] and finally mobile ANs and mobile UNs [36]. Because of the wide application, this work considers the scenarios of 'static ANs and static UNs' and 'mobile ANs and static UNs'.

Another classification of localization techniques is based on connectivity between ANs and UNs. Firstly, localization is categorized as classical and soft computing technique assisted schemes. Further, classical schemes are categorized as range based and range free techniques. The angle or distance data between server nodes is required in range-based schemes to obtain node position. Once this data is available, UN localization is performed using geometrical operations such as multilateration and angulation respectively if distance and angle statistics are available. Range-free methods require topological information unlike range-based methods. Range-based methods involve supplementary hardware complexity and thus these methods are reliable than range-free methods [37]. Angle of arrival (AoA) [38], time of arrival (ToA) [39], time difference of arrival (TDoA) [40], acoustic energy [41], and received signal strength indicator (RSSI) [42], [43] are some of the range-based methods. The RSSI schemes require deployment of an extra radio frequency (RF) antenna in each sensor node. The AoA scheme needs placement of additional antennas in a proper direction. All the receiving sensor nodes need to be perfectly synchronized in the ToA and TDoA schemes. Thus, as the range-based schemes require additional hardware, these schemes are complex over range-free schemes.

The range-free schemes operate based on pattern or hop count information. Hence, the hardware complexity of range free schemes is minimal at the cost of limited localization accuracy. The centroid algorithm [44], DV–hop technique [45], and geometric constraint algorithm [46] are some examples of range free schemes. The centroid algorithm allows UNs to convey proximity information to ANs and then UNs are localized to the centroid of the ANs. The DV–Hop algorithm and amorphous algorithm localize UNs with the hop count information and hop distance information, respectively instead of distance information. The range-based and range-free methods thus clearly differ in terms of localization accuracy and deployment cost [47]. Hence, metaheuristic search assisted localization (MSL) has been proposed to balance this trade-off amongst localization precision and deployment

cost [48], [49]. The gradient techniques like Gauss-Newton algorithm has a possibility of trapping local minima while optimizing MSL technique. Also, gradient schemes need approximate initial solutions of required parameters and differentiable cost functions [50]. The metaheuristic optimization techniques (MOTs) can become an appropriate substitute to gradient techniques as the MOTs start the search process with random initial parameters [51]. Various MOTs such as sequential greedy optimization [52], krill herd optimization [53], swarm based optimization [54], [55] and differential evolution (DE) [56], [57] algorithms are applied to MSL problem to achieve better localization accuracy. However, all these MSL techniques hardly handle non-linear distortion imposed in a wireless environment which is assumed to be log normal shadow-fading model (LNSM). Under such nonlinear environments, artificial neural network (ANN) architectures are appropriate substitutes. The multilayer perceptron (MLP) and radial basis function (RBF) networks are renowned models in the family of NNs because of their highly non-linear architectures. The MLP model is able to map input and output space with non-linear boundaries, whereas RBF network classifies the similar group of input data space in the form of ellipse or hyper spheres. The MLP based localization techniques are discussed in the literature [58], [59], [60] and RBF based localization is discussed in [61]. The RBF model is slightly better than MLP since the RBF uses Gaussian activation, which is more suitable for the systems suffering from Gaussian variables [62].

Recent developments also initiated the MAAN based localization in low power UAVs. From the literature survey of ground AN based localization, it is observed that soft computing techniques have a prominent role in node localization. Thus, the soft computing techniques such as OTs and NNs are also applied for MAAN based localization. The DE algorithm is one of the efficient OT. However, its convergence speed is still low as it is delicate to the selection of parameters like mutation factor and crossover probability. To increase convergence speed an adaptive DE (ADE) algorithm is proposed for the MSL problem [63]. ADE automatically updates cross over probability and mutation factor. Similarly, the artificial bee colony (ABC) process with innovative exploration and exploitation ability is also applied for MSL for better accuracy [64]. Further, a highly non-linear MLP and RBF based node localization is suggested for the MAAN system in [65] and [66] respectively. The MLP and RBF models need certainly huge training data sets. Thus, these models are replaced by the Extreme Learning Machine (ELM) due to its fast and strong learning abilities. Due to such rapid training ability, the ELM is used for MAAN based localization in [67]. Thus, a comparative analysis is made in this review paper amongst various soft computing based localization methods while using both FTAN and MAAN in a WSN.

The present review paper is prepared as follows. The localization system model for a WSN with MAAN deployed in UAV is presented in Section II. Section III and Section IV include respectively the MSL and NN based localization

TABLE 1. List of notations.

Parameter	Description
h_{opt}	Optimal height of UAV
(x_m^o, y_m^o)	True coordinate of mth UN
$(\hat{x}_m, \hat{y}_m)$	Estimated coordinate of mth UN
(x_q, y_q)	Spatial coordinate of UAV located at q^{th} waypoint
M	Number of UNs
D	Ground sensor field dimension
Q	Number of trajectory points
NS	Network area size in $(X \times Y)$ meters
P_0	The RSS value at reference distance d_0
d_{qm}	The true distance between m^{th} UN and UAV located at q^{th} trajectory point
$\hat{d}_{qm}$	The estimated distance between m^{th} UN and UAV located at q^{th} trajectory point
γ	The path loss exponent
X_σ	Gaussian random variable denoting log normal shadow–fading effect
$\hat{r}_{qm}$	The estimated distance between m^{th} UN and q^{th} spatial coordinated of UAV
$\hat{S}_m$	Estimated location if m^{th} UN using RSSI
P_d, G	Number of populations and generations in ADE
P_d, I_{max}	Number of populations and iterations in ABC
$\boldsymbol{w}, \boldsymbol{u}, \boldsymbol{v}$	Target, trail and mutant weight vectors of ADE
$\boldsymbol{a}, \boldsymbol{b}$	Target and neighbourhood weight vectors of ABC
F^g	Adaptive mutation factor of ADE in g^{th} generation
C_P^g	Adaptive crossover probability of ADE in g^{th} generation
$\hat{r}_m$	Input vector of MLP, RBF and ELM
H_M, H_R, H_E	Number of hidden nodes of MLP, RBF and ELM
U_{hq}	The weight of the connection between h^{th} hidden node and q^{th} input node of MLP
V_{lh}	The weight of the connection between l^{th} output node and h^{th} hidden node of MLP
W_{lh}	The weight of the connection between l^{th} output node and h^{th} hidden node of RBF
C_h	$(Q \times 1)$ dimensional centre vector of RBF
σ_h	Spread of the hth hidden neuron of RBF
$\boldsymbol{\alpha}_h$	The connection weights between all input nodes and h^{th} hidden neuron of ELM
$\boldsymbol{\beta}_h$	The connection weights between h^{th} hidden neuron and both the output nodes of ELM.
bi_h	Bias of hth hidden node of ELM

methods. Section V provides simulation results and analyses. Finally, this review paper concludes in Section VI with major findings.

Notations: This research review paper compares various soft computing techniques to localize UNs with the help of UAV. Thus, various parameters adopted in all these soft computing techniques are summarized in Table 1.

II. SYSTEM MODEL FOR UAV BASED LOCALIZATION
The MAAN–based localization model is shown in Fig. 1, where M UNs are installed in a 2–dimensional (2D) ground
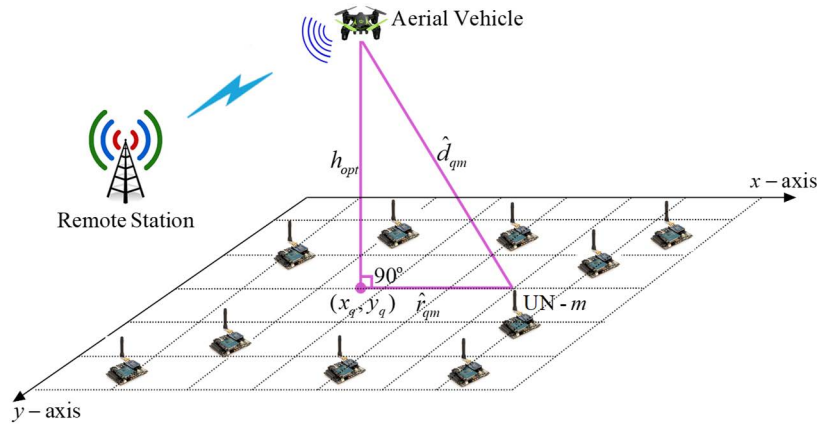
FIGURE 1. Architecture of UAV supported wireless sensor network [65], [67].
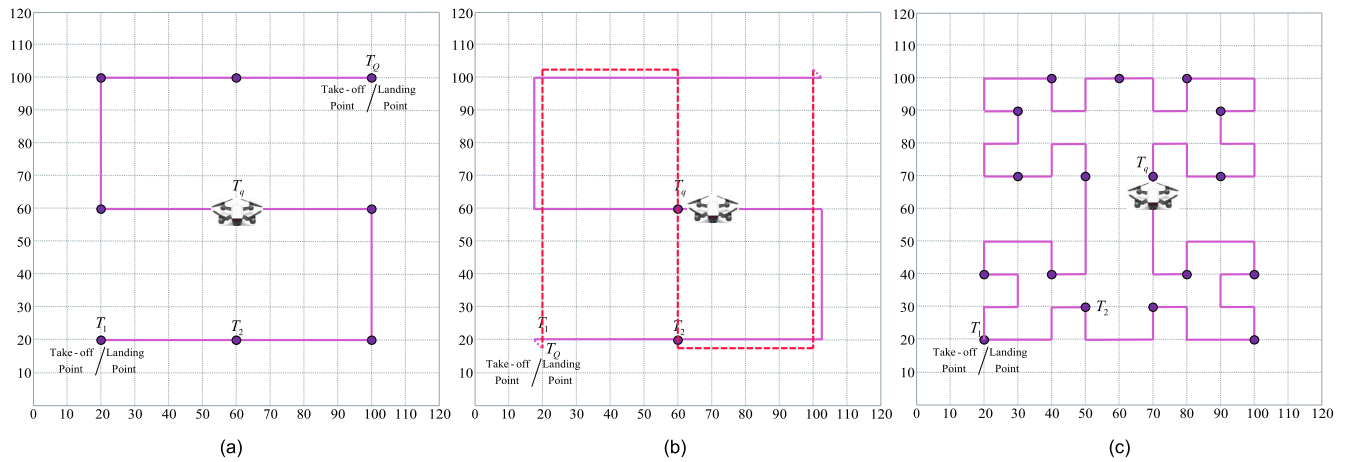

FIGURE 2. Trajectories of UAV in a 2D sensor field (a) SCAN (b) DOUBLE SCAN (c) HILBERT [67].

sensor field and a single MAAN is deployed in a UAV flying at the optimal height h_{opt}. The MAAN is assumed to know their positions (coordinates) and UNs are unaware of their positions. The position-aware MAAN is used to find positions of UNs in the localization procedure. The single MAAN deployed in a UAV acts as many virtual MAANs when the UAV is at different locations. The UAV moves with a specified speed and connects with the UNs with a definite broadcasting frequency. The UAV is set to fly in a specific trajectory from the take-off point to the landing point to cover the entire sensor field. Some examples of trajectories are SCAN, DOUBLE-SCAN and HILBERT as shown in Fig. 2. Among various trajectories depicted in this figure, the 'SCAN' trajectory provides uniform coverage to all UNs as shown in Fig. 2 (a). The SCAN trajectory includes huge collinear trajectory points. To avoid this problem, DOUBLE-SCAN is proposed, where the given sensor field is scanned in both horizontal and vertical directions, as shown in Fig. 2 (b). The DOUBLE-SCAN needs the MAAN to travel twice the distance as in the SCAN. However, the HILBERT trajectory shown in Fig. 2 (c), provides more non-collinear AN

trajectory points as compared to SCAN and DOUBLE-SCAN trajectories while localizing UNs. Among these three trajectories, the SCAN trajectory offers minimum localization error with minimum distance travel when the MAAN travels in the given sensor field with good resolution. The HILBERT trajectory provides minimum localization error when the resolution is more than the communication range. However, most of the literature considers SCAN trajectory for its minimum travel distance and satisfactory accuracy. It is assumed that all nodes can communicate with each other as all nodes are placed within the communication visibility. Each UN is also assumed to have distance from all ANs through RSS measurement recorded at each UN. Let $(\tilde{x}_m, \tilde{y}_m)$ and (x_q, y_q) are the true coordinates of mth UN and coordinates of projection of UAV located at q^{th} trajectory point, respectively. Then, the distance between MAAN placed at q^{th} trajectory point and m^{th} UN is obtained from the RSS value recorded at m^{th} UN. The RSS value recorded in LNSM is given by [65]:

$$RSS[d_{qm}]\,dBm = P_0[d_0]\,dBm - 10\gamma \log_{10}\left[\frac{d_{qm}}{d_0}\right] - X_\sigma$$

$$(1)$$

where P_0 is the RSS value at reference distance d_0, d_{qm} is the actual distance amongst m^{th} UN and MAAN located at q^{th} trajectory point and γ is the path loss exponent. The log normal shadow–fading effect is denoted by X_σ, which is a Gaussian random variable with zero mean and σ^2 variance. The estimated distance $\hat{d}_{qm}$ is measured from the RSS value given in (1) as [65]:

$$\hat{d}_{qm} = d_0 10^{\left[\frac{P_0[d_0] - RSSI[d_{qm}]}{10\gamma}\right]}, \quad q = 1, 2, \ldots, Q \quad (2)$$

The flying height of the UAV is a significant factor that affects localization accuracy. In general, environmental absorptions decrease as the height of UAV increases because of the availability of a better LoS path. Localization error increases gradually, beyond the optimal height. Thus, the flying height of an aerial vehicle has to be optimized first. Let, (x_q, y_q) be the coordinates of the projection of the UAV located at q^{th} trajectory point and $\hat{d}_q$ is the estimated distance between the UAV and the known reference node $(\tilde{x}_r \ \tilde{y}_r)$, which is generally deployed at the midpoint of the sensor area for computational simplicity. Then, the distance from the projection of UAV on the terrestrial sensor field to the reference node is computed as [67]:

$$r_q = \sqrt{(x_q - x_r)^2 + (y_q - y_r)^2} \quad (3)$$

Using the distance r_q, the optimal UAV flying height in the range between minimum height $h_{\min}$ and maximum height $h_{\max}$ is conveyed as the least square problem according to [67]:

$$h_{opt} = \arg \min_{h \in (h_{\min}, h_{\max})} \left[\sqrt{\sum_{q=1}^{Q} \left|\sqrt{\hat{d}_q^2 - h^2} - r_q\right|^2}\right] \quad (4)$$

Once the optimal height is obtained, the coordinates of mth UN, that is $(\tilde{x}_m, \tilde{y}_m)$, are computed using a multilateration procedure. Let the distance measurements from all UAV trajectory point projections to m^{th} UN be [66]:

$$(x_1 - \tilde{x}_m)^2 + (y_1 - \tilde{y}_m)^2 = \hat{r}_{1m}^2$$
$$(x_2 - \tilde{x}_m)^2 + (y_2 - \tilde{y}_m)^2 = \hat{r}_{2m}^2$$
$$\vdots$$
$$(x_Q - \tilde{x}_m)^2 + (y_Q - \tilde{y}_m)^2 = \hat{r}_{Qm}^2 \quad (5)$$

where $\hat{r}_{qm}^2 = \hat{d}_{qm}^2 - h_{opt}^2$. The set of equations given in (5) is easily solved by writing them in a linear form to the variables $\tilde{x}_m$ and $\tilde{y}_m$. Thus, subtracting the last equation from all previous equations yields [66]:

$$2(x_1 - x_Q)\tilde{x}_m + 2(y_1 - y_Q)\tilde{y}_m$$
$$= \hat{r}_{Qm}^2 - \hat{r}_{1m}^2 + x_1^2 - x_Q^2 + y_1^2 - y_Q^2$$
$$2(x_2 - x_Q)\tilde{x}_m + 2(y_2 - y_Q)\tilde{y}_m$$

$$= \hat{r}_{Qm}^2 - \hat{r}_{2m}^2 + x_2^2 - x_Q^2 + y_2^2 - y_Q^2$$
$$\vdots$$
$$2(x_{Q-1} - x_Q)\tilde{x}_m + 2(y_{Q-1} - y_Q)\tilde{y}_m$$
$$= \hat{r}_{Qm}^2 - \hat{r}_{Q-1m}^2 + x_{Q-1}^2 - x_Q^2 + y_{Q-1}^2 - y_Q^2 \quad (6)$$

In (6), let $S_m = [\tilde{x}_m \ \tilde{y}_m]^T$

$$A = 2 \begin{bmatrix} (x_1 - x_Q) & (y_1 - y_Q) \\ (x_2 - x_Q) & (y_2 - y_Q) \\ & \vdots \\ (x_{Q-1} - x_Q) & (y_{Q-1} - y_Q) \end{bmatrix}$$

and

$$B = \begin{bmatrix} \hat{r}_{Qm}^2 - \hat{r}_{1m}^2 + x_1^2 - x_Q^2 + y_1^2 - y_Q^2 \\ \hat{r}_{Qm}^2 - \hat{r}_{2m}^2 + x_2^2 - x_Q^2 + y_2^2 - y_Q^2 \\ \vdots \\ \hat{r}_{Qm}^2 - \hat{r}_{Q-1m}^2 + x_{Q-1}^2 - x_Q^2 + y_{Q-1}^2 - y_Q^2 \end{bmatrix},$$

then the position of mth UN is obtained from [66]:

$$\hat{S}_m = \left(A^T A\right)^{-1} A^T B \quad (7)$$

III. METAHEURISTIC SEARCH ASSISTED LOCALIZATION (MSL) TECHNIQUES

The precision of the RSS localization is subjected to the accuracy of distance measurement between UNs and ANs. This distance is computed according to the RSS recorded at UNs through the classical LNSM. However, this distance measurement is not accurate because of the distortions in LNSM. The location obtained by the RSS multilateration using such inaccurate distances is also not accurate. To improve the accuracy of the RSS technique, the localization problem is defined as an MSL problem. Thus, the MSL problem for the MAAN system to determine coordinates of mth UN($\hat{x}_m \ \hat{y}_m$) using distance measurements $\hat{r}_{qm}$ is defined as [63]:

$$(\hat{x}_m \ \hat{y}_m)$$
$$= \arg \min_{(\tilde{x}_m \ \tilde{y}_m)} \left[\sum_{q=1}^{Q} \left(\sqrt{(x_q - \tilde{x}_m)^2 + (y_q - \tilde{y}_m)^2} - \hat{r}_{qm}\right)^2\right] \quad (8)$$

where $m = 1, 2, \ldots, M$. The MSL problems defined in (8) can be optimized efficiently with popular OTs such as ADE and ABC algorithms.

A. ADE ASSISTED MSL TECHNIQUES
In the family of OTs, the DE algorithm is the popular technique that is used for optimizing several problems [68]. The DE algorithm has several similarities with the genetic algorithm (GA) [69]. Both of these two techniques are population-based and use the same operations like initialization, cross-over, mutation and selection. The DE processes its operations in a decimal format unlike the GA, which processes its operations in binary format. Thus, GA requires

an additional algorithm to convert binary entities into decimal entities. The DE algorithm became popular as it determines the optimal solution irrespective of its initial parameter and it uses limited control parameters. The DE algorithm tries to optimize the given problem iteratively and finds the optimal solution. This algorithm uses a mutation process for exploring solution space and a selection process to exploit solution space for the optimal solution. However, the convergence speed and performance of the DE algorithm depend on the selection of cross-over probability and mutation factor. Improper selection of these parameters may result either in poor performance or in low convergence speed. Thus, the ADE algorithm is suggested which has a self-adaptive strategy to select cross-over probability and mutation factor in each generation [70]. The ADE algorithm exhaustively explores solutions in the early generations and exploits more optimal solutions in the last few generations. The ADE assures an enhanced solution and also offers great convergence speed over the DE algorithm. Thus, the ADE algorithm has been applied to several optimization problems [71], [72]. Moreover, due to the merits of ADE over simple DE, the DE-assisted MSL technique proposed in [56] and [57] is modified as ADE-assisted MSL technique in [63]. ADE method includes main stages such as initialization, mutation, crossover and selection. The brief localization process is explained as follows [63].

In the initialization stage of ADE, a population of P_d individuals is randomly initialized. Each individual consists of two variables representing x and y locations of mth UN. The randomly initialized p^{th} population $\mathbf{w}_m$ is denoted as [63]:

$$\mathbf{w}_m^{g,p} = \left[x_m^{g,p}, y_m^{g,p}\right]^T, \quad p = 1, 2, \ldots, P_d, \quad g = 1, 2, \ldots, G \tag{9}$$

where m refers to the index of the UN and g refers to the index of generations. Mutation discovers the search area using an adaptive mutation factor F and the mutant vector $v_m^{g,p}$ is obtained from three mutually different individuals $\mathbf{w}_m^{g,r_1}$, $\mathbf{w}_m^{g,r_2}$ and $\mathbf{w}_m^{g,r_2}$, where $r_1, r_2, r_3 \in \{1, 2, \ldots, P_d\}$ as [63]:

$$v_m^{g,p} = \mathbf{w}_m^{g,r_1} + F(\mathbf{w}_m^{g,r_2} - \mathbf{w}_m^{g,r_3}) \tag{10}$$

Crossover is used to improve the range of initial vectors. Crossover creates a trial vector $\mathbf{u}_m$ by replacing some parameters of the vector $\mathbf{w}_m$ with randomly selected parameters of vector $\mathbf{v}_m$. The trail vector obtained from the cross-over operation is [63]:

$$\mathbf{u}_m^{g,p,d} = \begin{cases} v_m^{g,p,d} & rand_d(0,1) \le C_p, \\ w_m^{g,p,d} & otherwise. \end{cases} \tag{11}$$

where d is equal to 1 or 2 corresponding to the x-axis position or y-axis position, respectively.

In each generation, the ADE adopts an adaptive mechanism for changing crossover probability C_p and mutation factor F to obtain an optimal solution with high convergence speed. The obtained adaptive mutation factor F^{g+1} and crossover

probability C_p^{g+1} in $(g+1)^{\text{th}}$ generation are [63]:

$$F^{g+1} = \begin{cases} F_1 + rand_1 F_2, & if \ rand_2 < \tau_1, \\ F^g, & otherwise \end{cases} \tag{12}$$

$$C_p^{g+1} = \begin{cases} rand_3, & if \ rand_4 < \tau_2, \\ C_p^g, & otherwise \end{cases} \tag{13}$$

where $rand_j \in \{1, 2, 3, 4\}$, are random numbers lying between 0 and 1. F and C_p are defined by the constants τ_1 and τ_2, respectively, in each generation. The section stage depends on the cost value of both trail and target vectors. Thus, the fitness values of both target and trail vectors are computed respectively according to [63]:

$$fw_m^{g,p} = \sum_{q=1}^{Q} \left(\sqrt{(x_q - w_m^{g,p,1})^2 + (y_q - w_m^{g,p,2})^2} - \hat{r}_{qm} \right)^2 \tag{14}$$

$$fu_m^{g,p} = \sum_{q=1}^{Q} \left(\sqrt{(x_q - u_m^{g,p,1})^2 + (y_q - u_m^{g,p,2})^2} - \hat{r}_{qm} \right)^2 \tag{15}$$

The ADE uses a greedy selection procedure, which compares the cost values of all individuals in the vectors $\mathbf{w}_m$ and $\mathbf{v}_m$. The population with minimum cost value is carried to the next generation. The other individual may be discarded according to [63]:

$$\mathbf{w}_m^{g+1,p} = \begin{cases} u_m^{g,p} & fu_m^{g,p} \le fw_m^{g,p}, \\ \mathbf{w}_m^{g,p} & otherwise \end{cases} \tag{16}$$

The entire process is reiterated from the mutation stage till the termination criterion is encountered.

The optimal position m^{th} UN is obtained from the best individual with minimum cost value in the last generation (G). The position of mth UN is computed from [63]:

$$(\hat{x}_m \ \hat{y}_m)$$
$$= \arg \min_p \left[\sum_{q=1}^{Q} \left(\sqrt{(x_q - w_m^{G,p,1})^2 + (y_q - w_m^{G,p,2})^2} - \hat{r}_{qm} \right)^2 \right] \tag{17}$$

where $p = 1, 2, \ldots, P_d$. The entire procedure is repeated to obtain locations of remaining $(M-1)$ nodes. The pseudo algorithm for ADE-based localization is given as follows:

B. ABC ASSISTED MSL TECHNIQUES
The artificial bee colony (ABC) method introduced by Karaboga [73] has become popular with its capability to find the optimal solution in recent years. This algorithm has an innovative exploration and exploitation strategy by mimicking the intellectual foraging actions of honey bees. ABC handles exploration and refinement tasks by classifying the swarm of bees as employed, onlooker and scout bees. The exploration of a solution is done by the employed and scout bees and the refinement of a solution is taken care of by

Algorithm 1 ADE Algorithm for Node Localization

Input: $Q, \hat{r}, D, NS, (x_q, y_q)$ for $q = 1, 2, \ldots, Q$

Output: Estimated location of mth UN $(\hat{x}_m \; \hat{y}_m)$

1:     Initialize G, P_d, F, C_p and target vector $\boldsymbol{w}_m = NS \times$ $\text{rand}(P_d, D)$

2:     **for** $g = 1 : G$ **do**

3:        **for** $p = 1 : P_d$ **do**

4:           Select three mutually different individuals $\boldsymbol{w}_m^{g,r_1}, \boldsymbol{w}_m^{g,r_2}$ and $\boldsymbol{w}_m^{g,r_2}$, where $r_1, r_2, r_3 \in \{1, 2, \ldots, P_d\}$

5:           Compute mutant vector $\boldsymbol{v}^{g,p}$ using (10)

6:           Compute trail vector $\boldsymbol{u}_m^{g,p}$ using (11)

7:           Update mutation factor F^{g+1} and crossover probability C_p^{g+1} according to (12) and (13) respectively

8:           Compute fitness value of target vector $fw_m^{g,p}$ and fitness value of mutant vector $fu_m^{g,p}$ using (14) and (15) respectively

9:           **if** $fu_m^{g,p} \leq fw_m^{g,p}$ **then**

10:             $\boldsymbol{w}_m^{g+1,p} \leftarrow \boldsymbol{u}_m^{g,p}$

11:           **else**

12:             $\boldsymbol{w}_m^{g+1,p} \leftarrow \boldsymbol{w}_m^{g,p}$

13:           **end if**

14:        **end for**

15:     **end for**

16:     Compute $fw_m^{G,p}, p = 1, 2, \ldots, P_d$ using (14) in the final generation G

17:     Find $p_{\min}$ that yields minimum fitness value in the final generation G, $p_{\min} \leftarrow \arg\min_p \left(fw_m^{G,p} \right)$

18:     Estimate location of mth UN: $(\hat{x}_m \; \hat{y}_m) \leftarrow \boldsymbol{w}_m^{G,p_{\min}}$

---

the onlooker bees. Thus, the ABC algorithm obtains optimal solution by skipping premature convergence [74], [75]. The process implemented for MAAN-assisted node localization using the ABC algorithm is described briefly as follows.

Initially, the ABC algorithm randomly initializes a population set containing P_a populations, where each papulation comprises two variables analogous to the x and y coordinates of mth UN. The pth population in the ith iteration is described as [64]:

$$\boldsymbol{a}_m^{i,p} = \left[x_m^{i,p}, y_m^{i,p} \right]^T, \quad p = 1, 2, \ldots, P_a, \quad i = 1, 2, \ldots, I_{\max} \tag{18}$$

where $x_m^{i,p}$ and $y_m^{i,p}$ are the randomly generated x and y coordinates within the sensor network size (NS) in *meters*. Every employed bee produces a new solution in the neighborhood of its current solution. Thus, the neighborhood vector is expressed as [64]:

$$b_m^{i,p} = a_m^{i,p} + \phi_p \left(a_m^{i,p} - a_m^{i,k} \right) \tag{19}$$

where ϕ_p is a random number with limits $-1 < \phi_p < 1$, and k is a randomly selected population index that is different from the current population p. The fitness values of both the target and neighborhood vectors are computed respectively according to [64]:

$$fa_m^{i,p} = \sum_{q=1}^{Q} \left(\sqrt{(x_q - a_m^{i,p,1})^2 + (y_q - a_m^{i,p,2})^2} - \hat{r}_{qm} \right)^2 \tag{20}$$

$$fb_m^{i,p} = \sum_{q=1}^{Q} \left(\sqrt{(x_q - b_m^{i,p,1})^2 + (y_q - b_m^{i,p,2})^2} - \hat{r}_{qm} \right)^2 \tag{21}$$

ABC uses a greedy selection strategy after generating new food positions [64].

$$\boldsymbol{a}_m^{i,p} = \begin{cases} \boldsymbol{b}_m^{i,p} & fb_m^{i,p} \leq fa_m^{i,p}, \\ \boldsymbol{a}_m^{i,p} & otherwise \end{cases} \tag{22}$$

The onlooker bees obtain data about the food source from the employed bees and compute the cost value ($fa_m^{i,p}$) according to (20). Then the onlooker bees pick a food source, proportional to the probability that depends on the nectar amount PB_p. The roulette wheel selection is used for this probability-based selection, which is mathematically expressed as [64]:

$$PB_p = \frac{fa_m^{i,p}}{\sum_{p=1}^{P} fa_m^{i,p}} \tag{23}$$

After this selection, a new position is produced by onlooker bees in the neighbourhood of its current food position according to (19). The fitness values of new and old positions are again evaluated and the food position with minimum fitness value is retained. If a food position is not improved after 'limit' number of iterations, which is a prefixed number, then the food position is considered to be abandoned. The scout bees are used to discover a new food position according to (18).

The whole procedure will be repeated from the selection of food source for employed bees stage till the termination criterion is met. After reaching the termination criterion, the best food position with minimum cost value is treated as the location of mth UN according to [64]:

$$(\hat{x}_m \; \hat{y}_m)$$
$$= \arg\min_p \left[\sum_{q=1}^{Q} \left(\sqrt{(x_q - a_m^{I_{\max},p,1})^2 + (y_q - a_m^{I_{\max},p,2})^2} - \hat{r}_{qm} \right)^2 \right] \tag{24}$$

The whole procedure is reiterated to find the locations of remaining $(M - 1)$ nodes. The pseudo algorithm for ADE-based localization is given as follows:

IV. NEURAL NETWORK MODELS FOR LOCALIZATION

The localization accuracy of the classical RSS and proposed MSL techniques is limited, because the distance measurement obtained in LNSM is noisy due to the non-linear distortion induced in the wireless channel. Thus, the position

---

Algorithm 2 ABC Algorithm for Node Localization

Input: Q, $\hat{r}$, Limit, D, NS, (x_q, y_q) for $q = 1, 2, \ldots, Q$

Output: Estimated location of mth UN ($\hat{x}_m$ $\hat{y}_m$)

1:     Initialize $I_{\max}$, P_a, F, C_p and target vector $\boldsymbol{a}_m = NS \times$ rand(P_a, D)

2:     **for** $i = 1$: $I_{\max}$ **do**
      % food source selection by employed bee

3:      **for** $p = 1$: P_a **do**

4:        Select ϕ_p and $\boldsymbol{a}_m^{i,k}$ where k is a randomly selected population index that is different from p

5:        Compute neighborhood vector $\boldsymbol{b}_m^{i,p}$ using (19)

6:        Compute fitness value of target vector $fa_m^{i,p}$ and fitness value of neighborhood vector $fb_m^{i,p}$ according to (20) and (21) respectively

7:        **if** $fb_m^{i,p} \leq fa_m^{i,p}$ **then**

8:          $\boldsymbol{a}_m^{i,p} \leftarrow \boldsymbol{b}_m^{i,p}$

9:        **end if**

10:      **end for**

11:     Compute probability of each food source using (23)
      % food source selection by onlooker bees

12:     Initialize $l = 1$

13:      **for** $p = 1$: P_a **do**

14:        Select food source $\boldsymbol{a}_m^{i,k}$ according Roulette wheel selection procedure using the probabilities obtained in Step-11

15:        Compute neighborhood vector $\boldsymbol{b}_m^{i,p}$ using (19)

16:        Compute fitness value of neighborhood vector $fb_m^{i,p}$ and fitness value of target vector $fa_m^{i,p}$ according to (20) and (21) respectively

17:        **if** $fb_m^{i,p} \leq fa_m^{i,p}$ **then**

18:          $\boldsymbol{a}_m^{i,p} \leftarrow \boldsymbol{b}_m^{i,p}$

19:        **else**

20:          $l \leftarrow l + 1$

21:        **end if**

22:        **if** $l = $ Limit

23:          New food position is determined by scout bees $\boldsymbol{a}_m^{i,p} \leftarrow NS \times$ rand (P_a, D)

24:        **end if**

25:      **end for**

26:     **end for**

27:     Compute $fa_m^{I_{\max}, p}$, $p = 1, 2, \ldots, P_a$ using (15) in the final iteration I_{max}

28:     Find $p_{\min}$ that yields minimum fitness value in the final iteration I_{max}, $p_{\min} \leftarrow \arg\min_p \left(fa_m^{I_{\max}, p} \right)$

29:     Estimate location of mth UN: $(\hat{x}_m$ $\hat{y}_m) \leftarrow \boldsymbol{a}_m^{I_{\max}, p_{\min}}$

---

estimate obtained from such noisy distance measurement is also not accurate. Thus, the use of highly non-linear NN structures is particularly needed for node localization under such non–linear systems. The standard NN architectures such as MLP, RBF and ELM are efficiently used for UAV aided

node localization. The well trained NNs are capable of finding coordinates of UNs instantly even if they move to a new position within the same sensor field, whereas the RSS and MSL techniques have followed their entire localization procedure to find location of new positions.

A. UAV ASSISTED NODE LOCALIZATION USING MLP

The multilayer perceptron (MLP) is a popular feed-forward NN architecture with highly non-linear classification ability [76]. The MLP architecture is an effective structure for non-linear signal classification among various NN models [77], [78]. Thus, MLP is used for complex classification tasks like channel equalization [79] and signal detection [80], [81], [82], [83]. The well-trained MLP model is applied effectively for node localization as it is also a classification task. The back propagation (BP) supervised learning algorithm is used for training weights of the MLP network [84]. The BP algorithm starts its working process by initializing network weights randomly and then the input data vector is supplied to the MLP to produce the output vector. The error vector is computed from the deviation between output and desired data signal vectors. This error vector is then fed back along the network to update connection weights.

The configuration of UAV-assisted node localization to find coordinates of mth UN using the MLP model is depicted in Fig. 3. The MLP architecture presented here contains Q input nodes, H_M hidden neurons and two output neurons. The x and y coordinates of mth UN are expected to be obtained from two output neurons. The number of input elements is chosen according to the number of virtual MAANs. The input elements and hidden neurons are coupled through weighted feed-forward connections. Similarly, hidden and output neurons are also coupled with weighted feed-forward connections. Each neuron in the hidden layer is designed with a simple summer and a non-linear activation function. Thus, the output of each hidden neuron is computed as [65]:

$$z_h = \phi \left(\sum_{q=1}^{Q} U_{hq} \hat{r}_{qm} \right), \quad h = 1, 2, \ldots, H_M \quad (25)$$

In the above equation, U_{hq} is the weight of the connection from h^{th} hidden node to q^{th} input node. The non-linear activation function ϕ is chosen according to requirement. In the present paper, the unipolar sigmoid function is used as an activation function. So $\phi(t) = 1/(1 + e^{-t})$.

There exists a connection weight V_{1h} for the connection from h^{th} hidden node to the first output node and a connection weight V_{2h} for the connection from h^{th} hidden node to the second output node. The two output neurons are treated as simple summers and the estimated x and y locations of mth UN are respectively computed from these neurons as [65]:

$$\hat{x}_m = \sum_{h=1}^{H_M} V_{1h} z_h \text{ and } \hat{y}_m = \sum_{h=1}^{H_M} V_{2h} z_h \quad (26)$$
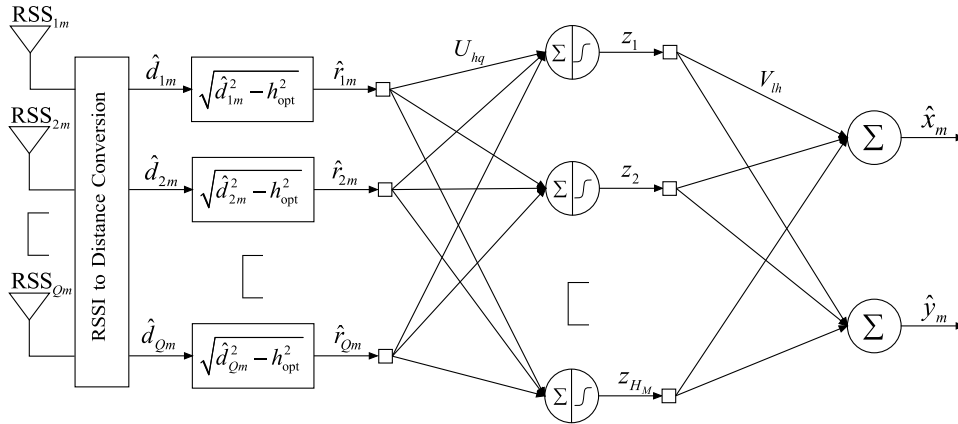
FIGURE 3. MLP model for UAV-assisted localization m[th] UN [65].

B. UAV ASSISTED NODE LOCALIZATION USING RBF

Another great variety of NN models is the Radial Basis Function (RBF) model, which has a high degree of nonlinearity during input data classification [85], [86]. The centre, spread, and the network weights are free parameters of this network. The RBF network can be used for highly non-linear classification problems upon the proper selection of these parameters and number of hidden neurons. The Gradient Descent (GD) algorithm is generally applied for training the free parameters of the RBF [87]. The GD algorithm that is used for network training computes response for the given input training data vector. Then, the error vector is computed from the variance between the RBF response vector and desired vector. This error vector is used to modify free parameters of the RBF network such as output weights, centres and spreads. The RBF model is widely used for several problems due to its complex nonlinear mapping and adaptive learning abilities [88], [89]. Since node localization in wireless sensor networks is also viewed as a pattern classification problem, the RBF model is also used for such node localization problems. The RBF with Gaussian activation is expected to be more suitable than the MLP during node localization as the log-normal shadow-fading effect of the wireless channel is also modelled with Gaussian random variables.

The RBF architecture for finding location of mth UN in a WSN using UAV is portrayed in Fig. 4. The RBF described in this figure comprises three layers namely input layer containing Q elements, hidden layer containing H_R neurons and output layer containing two neurons. These neurons in the output layer give x and y locations of mth UN. The number of input elements is equal to the number of virtual MAANs. There exist imaginary connections between input and hidden nodes. Since the imaginary connections do not carry any weights, the data from the input layer is directly transferred to the hidden layer. However, the hidden and output nodes are coupled with weighted connections. Hence, the weighted hidden layer outputs are transferred to the output layer.

The RBF model for node localization has hypothetical input weights. Since these connections do not carry any weights, the input vector $\hat{\boldsymbol{r}}_m$ directly appears at the hidden layer. Since the hidden neurons consist of Gaussian activation, the output from each hidden neuron is represented as [66]:

$$z_h = \exp\left(-\frac{\|\hat{\boldsymbol{r}}_m - \boldsymbol{C}_h\|^2}{2\sigma_h^2}\right), \quad h = 1, 2, \ldots, H_R \quad (27)$$

where $\hat{\boldsymbol{r}}_m = [\hat{r}_{1m}, \hat{r}_{1m}, \ldots, \hat{r}_{Qm}]^T$, $\boldsymbol{C}_h$ is the $(Q \times 1)$ dimensional center vector and σ_h is the spread of the hth hidden neuron. Similar to MLP, there exists a connection weight W_{1h} for the connection from h[th] hidden node to the first output node and a connection weight W_{2h} for the connection from h[th] hidden node to the second output node. Since the two output neurons have simple summers, the x and y coordinates of mth UN are computed respectively from both the output neurons as [66]:

$$\hat{x}_m = \sum_{h=1}^{H_R} W_{1h}z_h \text{ and } \hat{y}_m = \sum_{h=1}^{H_R} W_{2h}z_h \quad (28)$$

C. UAV ASSISTED NODE LOCALIZATION USING ELM

Though the NN models such as MLP and RBF attain satisfactory localization accuracy, their training speed is the major bottleneck for practical implementation. The MLP and RBF models require huge training data sets to train the networks. Thus, the ELM proposed by Huang can substitute MLP and RBF models due to its fast and strong learning ability during network training [90]. ELM contains only a single hidden layer between input and output layers. The input connection weights from input to output layers are randomly initialized and the output connection weights from hidden to output layers are selected methodically in a single step [91]. This kind of analytical selection of output weights avoids users spending much time on training a network. Thus, the ELM has fast training speed and it also has much better performance
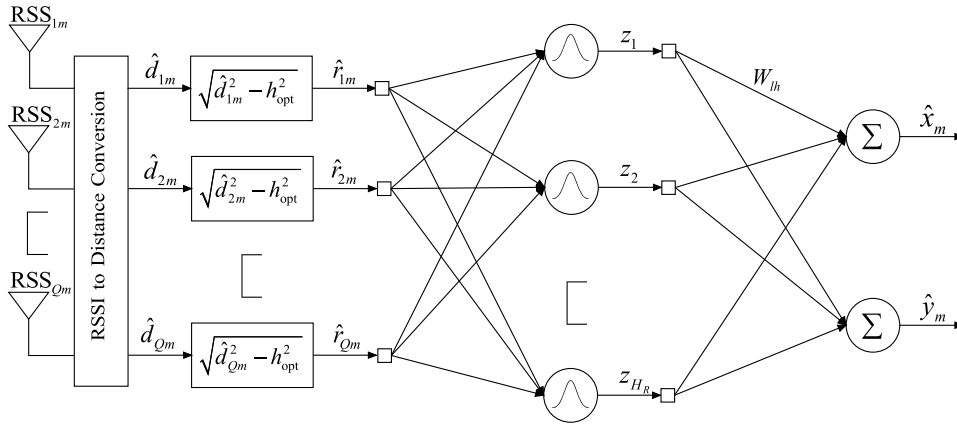
FIGURE 4. RBF model for UAV-assisted localization of mth UN [66].

through its strong learning ability. Due to these abilities, the ELM has numerous applications [92], [93], [94]. The ELM architecture for finding location of mth UN in WSN using UAV is depicted in Fig. 5. The ELM presented here consists of Q input nodes, H_E hidden neurons and two output nodes. The vector of distances from projections of all UAV trajectory points on ground sensor field to m^{th} UN deployed on the same sensor field is considered to be input vector. The two output nodes compute x and y location of mth UN. Thus, the input vector $\hat{r}_m = [\hat{r}_{1m}, \hat{r}_{2m}, \ldots, \hat{r}_{Qm}]^T \in R^Q$, and the output vector $[\hat{x}_m, \hat{y}_m]^T \in R^2$ of the ELM are precisely mapped as [67]:

$$\sum_{h=1}^{H_E} \beta_h g\left(\alpha_h^T \hat{r}_m + bi_h\right) = [\hat{x}_m, \hat{y}_m]^T, \quad m = 1, 2, \ldots, M \tag{29}$$

where $g(\hat{r})$ denote the non-linear activation function. Unipolar sigmoid is the most preferred activation. Further, $\alpha_h = [\alpha_{1h}, \alpha_{2h}, \ldots, \alpha_{Qh}]^T$ represents connection weights between the input signal vector and h^{th} hidden neuron, $\beta_h = [\beta_{h1}, \beta_{h2}]^T$ represents connection weights between h^{th} hidden neuron and both the output nodes and bi_h indicates a bias of hth hidden neuron.

The ELM is trained to match the target vector, $[\tilde{x}_i^t, \tilde{y}_i^t]^T$ by feeding input training vectors $\hat{r}_i^t = [\hat{r}_{1i}^t, \hat{r}_{2i}^t, \ldots, \hat{r}_{Qi}^t]^T$ where $i = 1, 2, \ldots, M_E$ and M_E represents the total number of training symbols. Similar to (29), the input and output training vectors are mathematically related as [67]:

$$\sum_{h=1}^{H_E} \beta_h g\left(\alpha_h^T \hat{r}_i^t + bi_h\right) = [\tilde{x}_i^t, \tilde{y}_i^t]^T, \quad i = 1, 2, \ldots, M_E \tag{30}$$

The matrix form of (30) is [67]:

$$H\beta = T \tag{31}$$

where

$$H = \begin{bmatrix} g\left(w_1^T \hat{r}_1^t + bi_1\right) & \cdots & g\left(w_{H_E}^T \hat{r}_1^t + bi_{H_E}\right) \\ \vdots & \vdots & \vdots \\ g\left(w_1^T \hat{r}_{M_T}^t + bi_1\right) & \cdots & g\left(w_{H_E}^T \hat{r}_{M_T}^t + bi_{H_E}\right) \end{bmatrix}_{M_E \times H_E}$$

$$\beta = \begin{bmatrix} \beta_{11} & \beta_{12} \\ \vdots & \vdots \\ \beta_{H_E 1} & \beta_{H_E 2} \end{bmatrix}_{H_E \times 2} \text{ and } T = \begin{bmatrix} \tilde{x}_1^t & \tilde{y}_1^t \\ \vdots & \vdots \\ \tilde{x}_{M_T}^t & \tilde{y}_{M_T}^t \end{bmatrix}_{M_E \times 2}$$

During network training, the ELM computes the output weights (β) using randomly initialized input connection weights (α) and hidden node biases (bi) by finding the least square solution of the linear equation $H\beta = T$, which is described according to [67]:

$$\beta = \arg\min_{\beta} \|H\beta - T\| \tag{32}$$

The solution to the least square problem given in (32) is [67]:

$$\beta = H^\dagger T, \text{ where } H^\dagger = (H^T H)^{-1} H \tag{33}$$

This single step of the training process guarantees minimum training time and appropriate learning. These trained output weights, random input weights and random hidden node biases are used to compute coordinates of mth UN according to (29).

V. SIMULATION RESULTS

In the simulation section, the localization accuracy of various techniques such as RSS, MSL, MLP, RBF and ELM are compared by the use of both FTANs and MAAN. In the present paper, we assumed deployment of 100 UN in a 2D sensor field of (120×120) square meters dimension. To eliminate ambiguity in the position estimates, all estimated locations are averaged for 100 runs. The simulation parameters of UAV are chosen by extensive experimentation as listed in Table 2. The parameters required to represent GG and AG channels are also presented in the same table [13], [14]. The parameters
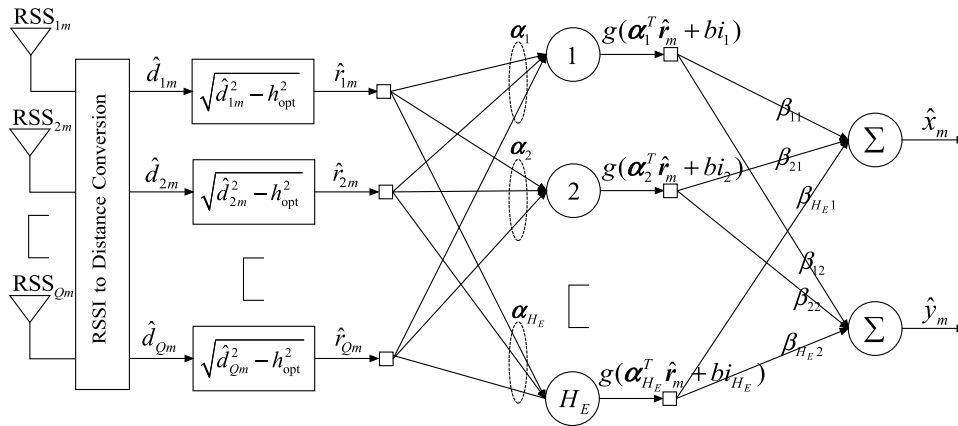
FIGURE 5. ELM model for m^{th} UN localization using UAV [65], [67].

TABLE 2. Simulation parameters of UAV and channel models.

Parameter	Value
UAV Parameters	
Broadcasting frequency	1/sec
UAV speed	40 m/s
h_{min} and h_{max}	20 m and 100 m
Optimal Flying height	41.663 m
AG Channel	
Reference distance (d_0)	1 m
Path-loss at reference distance $(P_0[d_0])$	− 34.906 dBm
Path-loss exponent (γ)	2.6533
Standard Deviation (σ)	2.15
GG Channel	
Reference distance (d_0)	1 m
Path-loss at reference distance $(P_0[d_0])$	− 30.446 dBm
Path-loss exponent (γ)	2.835
Standard Deviation (σ)	5.3

TABLE 3. Simulation parameters of MSL and NN models.

Parameter	Value
ADE	
Number of Generation (G)	20
Population Size (P_d)	20
Initial Cross-over Probability (C_P)	0.6
Initial Mutation Factor (F)	0.5
$[\tau_1, \tau_2, F_1, F_2]$	[0.1, 0.1, 0.1, 0.9]
ABC	
Number of iterations (I_{max})	20
Papulation Size (P_a)	20
Limit $(L = 0.6 \times I_{max} \times D)$	24
NN Models	
Number of input nodes (Q)	9
Number hidden neurons (H_M), (H_R) and (H_E)	18
Number of output neurons (D)	2
Weight Learning rate of MLP (μ)	0.08
Learning parameters of RBF $[\mu_w, \ \mu_c, \mu_s]$	[0.08, 0.05, 0.06]
Number of training symbols for MLP and RBF (M_T)	10000
Number of training symbols for ELM (M_E)	2000

of ADE and ABC-based MSL and NN techniques are listed in Table 3.

The performance measures such as average localization error (ALE), root mean square error (RMSE) and m^{th} node localization error (LE_m) are used to evaluate performance of various techniques as expressed respectively as follows [65]

$$ALE = \frac{1}{M} \sum_{m=1}^{M} \sqrt{(\hat{x}_m - \tilde{x}_m)^2 + (\hat{y}_m - \tilde{y}_m)^2} \quad (34)$$

$$RMSE = \sqrt{\frac{1}{M} \sum_{m=1}^{M} (\hat{x}_m - \tilde{x}_m)^2 + (\hat{y}_m - \tilde{y}_m)^2} \quad (35)$$

$$LE_m = \sqrt{(\hat{x}_m - \tilde{x}_m)^2 + (\hat{y}_m - \tilde{y}_m)^2} \quad (36)$$

where $(\tilde{x}_m, \tilde{y}_m)$ and $(\hat{x}_m, \hat{y}_m)$ are the actual and estimated positions of mth UN respectively.

TABLE 4. Performance comparisons of RSS localization for various UAV trajectories.

Trajectory	Number of Trajectory Points	Distance Covered in meters	ALE in meters
SCAN	9	320	2.9697
DOUBLE SCAN	17	640	2.3369
HILBERT	17	680	2.1351

Firstly, the ALE values obtained using RSS for different UAV trajectory paths are presented in Table 4. It is observer from this table is that the ALE of HILBERT trajectory is minimum because this path offers more trajectory points through longest distance travel. On the other hand, SCAN
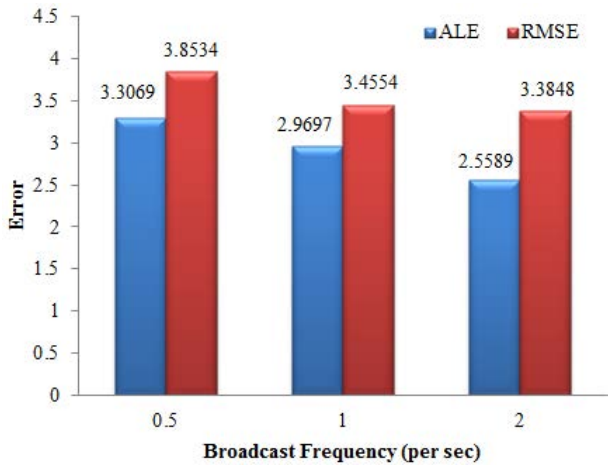
FIGURE 6. Localization accuracies for different broadcat frequencies [65], [67].

TABLE 5. ALE and RMSE of various localization schemes.

Localization Technique	FTANs		MAAN	
	ALE	RMSE	ALE	RMSE
RSS	4.9845	6.2561	2.8993	3.4554
ADE	2.1984	2.5407	1.6911	2.0184
ABC	2.0788	2.4901	1.6441	1.9019
MLP	1.1009	1.3272	0.9261	1.1352
RBF	1.0482	1.2822	0.8571	1.0474
ELM	0.7444	0.8992	0.3763	0.4426

TABLE 6. Complexities required for various localization techniques.

Technique	Complexity Order	Numerical Complexity
ADE	$G \times P_d \times M$	4×10^4
ABC	$I_{max} \times P_a \times M$	4×10^4
MLP	$M_T + M$	1.01×10^4
RBF	$M_T + M$	1.01×10^4
ELM	$\approx M$	100

trajectory leaves little high ALE, but not bad as compared to HILBERT trajectory. The SCAN trajectory achieves this ALE with a very less number of trajectory points compared to HILBERT trajectory. The DOUBLE SCAN trajectory has an intermediate performance between SCAN and HILBERT trajectories. Since there is not much improvement in ALE using HILBERT trajectory and also since SCAN trajectory has less number of trajectory points, we have chosen SCAN trajectory for the rest of our simulations. Additionally, since the longest travel also imposes extra energy consumption, the SCAN trajectory is selected as it travels the shortest distance.

The localization error of RSS–multilateration is computed as shown in Fig. 6 when the UAV is flying in SCAN trajectory at a height of 41.663 meters and broadcasting signals at frequencies 0.5, 1 and 2. The flying height is obtained through height optimization problems. The localization error is measured in terms of ALE and RMSE. It is witnessed from this figure that the localization error becomes lesser for higher broadcasting frequency because the higher broadcasting frequency arranges more virtual ANs. The UAV traveling at 40 m/s results in 5, 9 and 17 numbers of virtual ANs for the broadcasting frequencies 0.5, 1 and 2, respectively. The localization error is the minimum for broadcasting frequency 2. However, the broadcasting frequency is chosen to be $1/s$ for the remaining simulations because localization error is not greatly deviated for broadcasting frequencies 1 and 2. Also, the computational complexity of broadcasting frequency $1/s$ is lesser than the broadcasting frequency $2/s$.

The localization accuracies in terms of both ALE and RMSE for various methods using both FTANs and MAAN are listed in Table 5. These results convey the efficacy of MAANs over FTANs. For example, the ALE and RMSE values attained by the ELM with 9 fixed ANs are 0.7444 m and 0.8992 m respectively, whereas the ALE and RMSE values attained by the same ELM with a single UAV are just 0.3763 m and 0.4426 m respectively. Thus, the MAAN offers better localization accuracy with minimum cost. It is

also found from this table that the ADE and ABC-based MSL techniques perform well over the poor RSS. The localization accuracy of MSL techniques is still not satisfactory due to the non-linear distortions induced in the wireless channels. Under such situations, the non-linear techniques such as MLP, RBF and ELM perform fairly well over the RSS and MSL techniques. The ALE of ELM is consistently outperforming all other techniques with an accuracy enhancement of (40–85) % over RBF, MLP, MSL and RSS schemes. Similarly, the RMSE of ELM has an accuracy enhancement of (42–87) % over RBF, MLP, MSL and RSS schemes. This performance improvement is attained in cases of both FTANs and MAAN as seen in Table 5.

The projections of UAV on terrestrial sensor area, true locations of UNs, and the computed locations of UNs using different localization techniques are illustrated in Fig. 7. From this figure, it is observed that the NN techniques are outperforming MSL techniques and the accuracy of ELM is high over RSSI, MSL, MLP and RBF techniques. Thus, we can observe that the true and estimated location using ELM almost coincide as we see in Fig. 7(f), whereas there exists a huge deviation between the true and estimated location of RSS as we can see in Fig. 7(a). This attribute is because the ELM has a high nonlinear structure with strong learning ability.

The localization error obtained for each UN using several localization methods with MAAN is illustrated Fig. 8. As perceived in this figure, the RSS results in significant deviation in localization error for different UNs as shown in Fig. 8(a) because the RSS scheme fails to estimate coordinates of UNs situated far away from all ANs. Unlike RSS, the MSL techniques result in less localization error for each
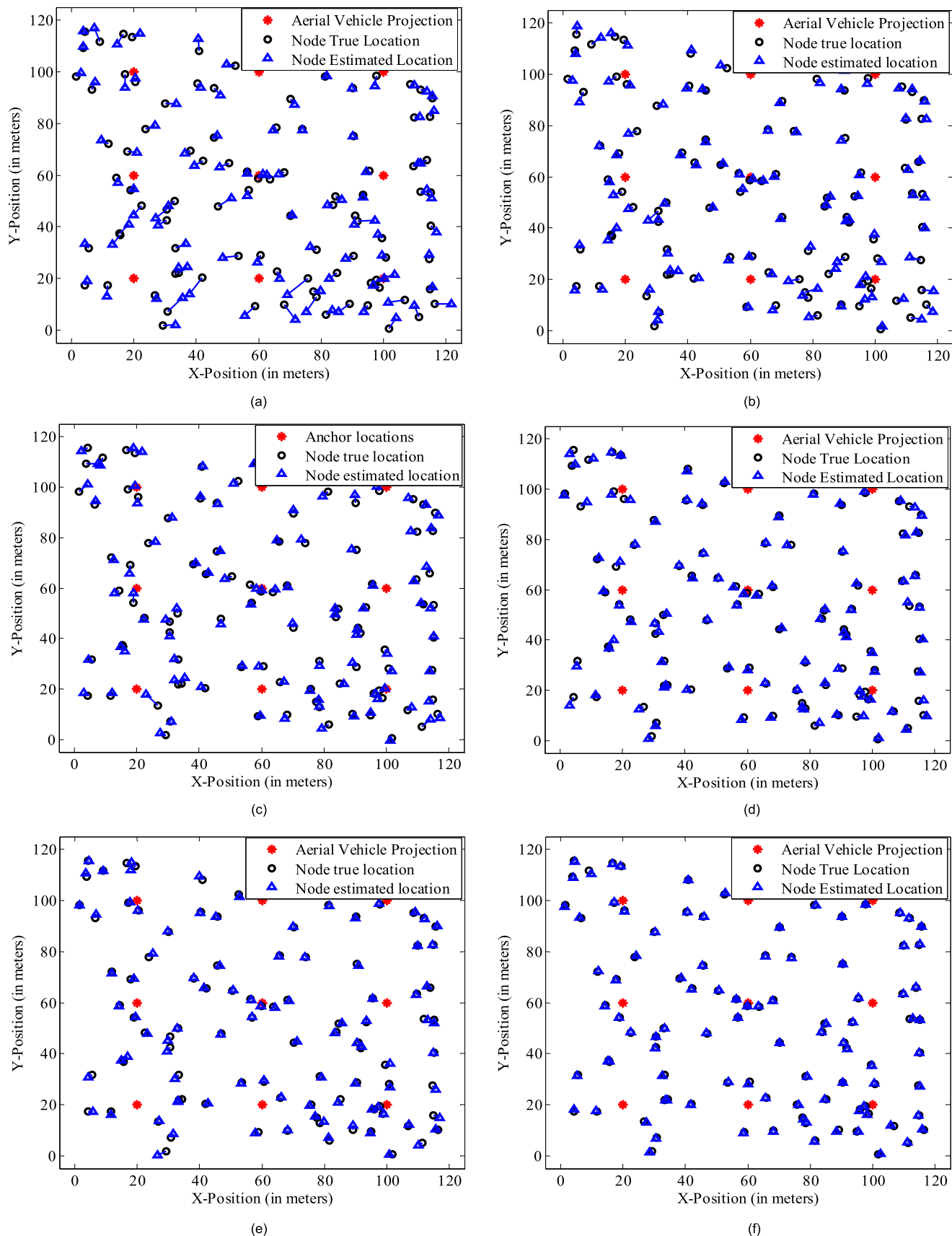
FIGURE 7. UAV assisted UN localization using: (a) RSS (b) ADE (c) ABC (d) MLP (e) RBF (f) ELM [65], [67].
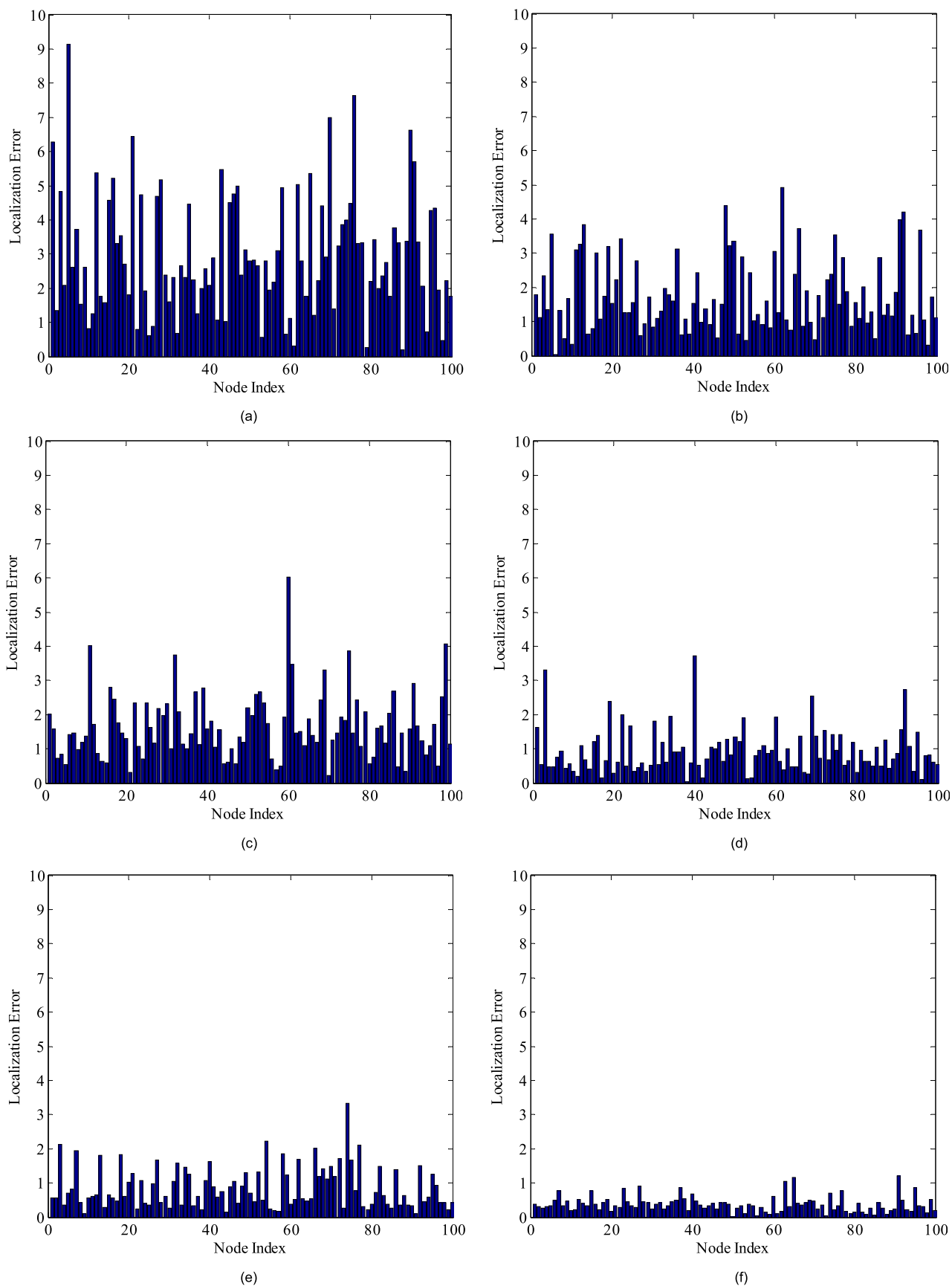
FIGURE 8. Localization error computed for each UN using various localization techniques: (a) RSS (b) ADE (c) ABC (d) MLP (e) RBF (f) ELM [65], [67].

TABLE 7. Comparison among various localization techniques based on their features.

Feature	RSSI [42]	ADE MSL [63]	ABC MSL [64]	MLP [65]	RBF [66]	ELM [67]
Performance	Poor	Sub–optimal	Sub–optimal	Near –optimal	Near–optimal	Optimal
Complexity	Very Less	High	High	Moderate	Moderate	Less
Mobility of UNs	Not Supports	Not Supports	Not Supports	Supports	Supports	Supports
Search time	Very Less	High	High	Moderate	Moderate	Very Less
Requirements	Extra receiving Antenna	Metaheuristic optimization	Metaheuristic optimization	Huge training data set	Huge training data set	Minimal training data set
Main Benefit	Low Complexity	Fast convergence with F and C_p	Capability to find optimal solution	Highly non-linear classification	Highly non-linear classification	Highly non-linear classification with fast and strong learning ability

FIGURE 9. Average localization error of various localization schees with increased number of UNs [65], [67].

depicted in Fig. 9. Furthermore, the MLP, RBF and ELM techniques have low localization error as compared to RSS and MSL techniques with an increased number of UNs.

The complexities required to localize M UNs have been made among various techniques as shown in Table 6. The numerical complexities computed for various techniques are as per the parameters presented in Table 2 and Table 3. In this work, the complexity denotes the number of cost function evaluations. In the present work, the MSL problem given in (8) is considered as a cost/fitness function. Further, to make an appropriate comparison between ADE and ABC algorithms, we have considered approximately equal complexity for both ADE and ABC algorithms. Thus, the complexities considered for both ADE and ABC algorithms are the same as seen in Table 6. On the other hand, the complexities in MLP, RBF and ELM techniques refer to the number of training symbols required. Table 6 also clearly declares that the MLP and RBF techniques have a substantial complexity gain over the MSL schemes. The ELM has further complexity gain over MLP and RBF as the ELM trains the network in a single iteration. From this table, it is also observed that the MSL scheme enforces exponentially increased complexity with an increased number of UNs. By contrast, the NN techniques need only linearly increased complexity.

Finally, Table 7 provides the brief comparison among various soft computing based localization schemes in terms of major features. Thus, this paper includes major finding of this paper and supports the usage of NN schemes.

UN because of their capability to find global optimal solution. The MLP, RBF and ELM schemes are able to find optimal positions for all UN irrespective of their locations due to their exhaustive training mechanisms. Thus, error distributions of these techniques are almost uninformed as observed in Fig. 8(d) to Fig. 8(f). Further, ELM has an edge over MLP and RBF as ELM results in localization error approximately below 2 m for all UNs as shown in Fig. 8(f), whereas some of the UNs localized by MLP and RBF occasionally yield localization error up to 4 m as shown in Fig. 8(d) and Fig. 8(e), respectively. This is due to the strong learning ability of ELM.

The ALE is computed for various localization methods while varying the number of UNs as presented in Fig. 9. Usually, the ALE in a highly dense network is lower than in a low dense network because the number of UNs under the proximity of each ANs increases as the number of UNs increases. The ALE decreases as the connectivity between ANs and UNs increases. Thus, the ALE of all localization techniques decreases with an increased number of UNs as

VI. CONCLUSION AND FUTURE SCOPE
Estimation of node coordinates is essential for many applications of WSNs. Node localization using FTANs suffers from poor localization accuracy and high execution cost because FTANs use unreliable GG channel link to estimate the location of a node. The MAAN deployed in UAV is preferred over FTAN to make the network more viable and to improve localization accuracy because MAANs uses reliable AG channel link to estimate the location of UNs. Among various localization techniques, soft computing techniques-based localization is preferred over the RSS-multilateration

because the RSS technique suffers from poor localization accuracy. Though the OT-assisted MSL schemes perform well over RSS, the non–linear distortions induced in the wireless channel limit their MSL's performance. Thus, the non–linear techniques such as MLP, RBF and ELM are considered to be better choices. Among these NN techniques, the ELM outperforms the MLP and RBF due to its fast and strong learning ability. The ELM approximately has an accuracy gain of (40–85) % over RBF, MLP, MSL and RSS schemes. NN-based schemes are also efficient as they support the mobility of UNs. The well-trained NNs are capable of finding the coordinates of UNs instantly even if they move to a new position within the same sensor field, whereas the RSS and MSL techniques follow their entire localization procedure to find location of new positions.

In the present work, we aimed to localize UNs deployed on 2–dimensional ground sensor fields using aerial ANs. However, in some circumstances, UNs may also be placed in 3–dimensional aerial environment instead of always placing them in a 2–dimensional ground plane. Since there exist several factors influencing the localization of aerial UNs, localization of such UNs placed on 3–dimensional plane would be an interesting and challenging task.

The present study estimates locations for virtual UNs in the ground sensor field. This study could be more challenging in future by considering the impacts of the natural phenomenas such as RSS values obtained through non LoS paths, energy requirements, acoustic emission, speed of the mobile UNs and so on.

REFERENCES

[1] M. A. Jamshed, K. Ali, Q. H. Abbasi, M. A. Imran, and M. Ur-Rehman, "Challenges, applications, and future of wireless sensors in Internet of Things: A review," *IEEE Sensors J.*, vol. 22, no. 6, pp. 5482–5494, Mar. 2022, doi: 10.1109/JSEN.2022.3148128.

[2] I. Khan, F. Belqasmi, R. Glitho, N. Crespi, M. Morrow, and P. Polakos, "Wireless sensor network virtualization: A survey," *IEEE Commun. Surveys Tuts.*, vol. 18, no. 1, pp. 553–576, 1st Quart., 2016, doi: 10.1109/COMST.2015.2412971.

[3] A. Boubrima, W. Bechkit, and H. Rivano, "Optimal WSN deployment models for air pollution monitoring," *IEEE Trans. Wireless Commun.*, vol. 16, no. 5, pp. 2723–2735, May 2017, doi: 10.1109/TWC.2017.2658601.

[4] W. Balid, H. Tafish, and H. H. Refai, "Intelligent vehicle counting and classification sensor for real-time traffic surveillance," *IEEE Trans. Intell. Transp. Syst.*, vol. 19, no. 6, pp. 1784–1794, Jun. 2018, doi: 10.1109/TITS.2017.2741507.

[5] K. Lorincz, "Sensor networks for emergency response: Challenges and opportunities," *IEEE Pervasive Comput.*, vol. 3, no. 4, pp. 16–23, Apr. 2004, doi: 10.1109/MPRV.2004.18.

[6] A. Pantelopoulos and N. G. Bourbakis, "A survey on wearable sensor-based systems for health monitoring and prognosis," *IEEE Trans. Syst., Man, Cybern., C, Appl. Rev.*, vol. 40, no. 1, pp. 1–12, Oct. 2010, doi: 10.1109/TSMCC.2009.2032660.

[7] J. Ko, C. Lu, M. B. Srivastava, J. A. Stankovic, A. Terzis, and M. Welsh, "Wireless sensor networks for healthcare," *Proc. IEEE*, vol. 98, no. 11, pp. 1947–1960, Nov. 2010, doi: 10.1109/JPROC.2010.2065210.

[8] M. Bertocco, G. Gamba, A. Sona, and S. Vitturi, "Experimental characterization of wireless sensor networks for industrial applications," *IEEE Trans. Instrum. Meas.*, vol. 57, no. 8, pp. 1537–1546, Aug. 2008, doi: 10.1109/TIM.2008.925344.

[9] K. Romer and F. Mattern, "The design space of wireless sensor networks," *IEEE Wireless Commun.*, vol. 11, no. 6, pp. 54–61, Dec. 2004, doi: 10.1109/MWC.2004.1368897.

[10] B. Spinelli, L. E. Celis, and P. Thiran, "A general framework for sensor placement in source localization," *IEEE Trans. Netw. Sci. Eng.*, vol. 6, no. 2, pp. 86–102, Apr. 2019, doi: 10.1109/TNSE.2017.2787551.

[11] G. M. Djuknic and R. E. Richton, "Geolocation and assisted GPS," *Computer*, vol. 34, no. 2, pp. 123–125, 2001, doi: 10.1109/2.901174.

[12] H. Chizari, T. Poston, S. Abd Razak, A. H. Abdullah, and S. Salleh, "Local coverage measurement algorithm in GPS-free wireless sensor networks," *Ad Hoc Netw.*, vol. 23, pp. 1–17, Dec. 2014.

[13] A. A. Khuwaja, Y. Chen, N. Zhao, M.-S. Alouini, and P. Dobbins, "A survey of channel modeling for UAV communications," *IEEE Commun. Surveys Tuts.*, vol. 20, no. 4, pp. 2804–2821, 4th Quart., 2018, doi: 10.1109/COMST.2018.2856587.

[14] C. Yan, L. Fu, J. Zhang, and J. Wang, "A comprehensive survey on UAV communication channel modeling," *IEEE Access*, vol. 7, pp. 107769–107792, 2019, doi: 10.1109/ACCESS.2019.2933173.

[15] B. Wang, Y. Sun, N. Zhao, and G. Gui, "Learn to coloring: Fast response to perturbation in UAV-assisted disaster relief networks," *IEEE Trans. Veh. Technol.*, vol. 69, no. 3, pp. 3505–3509, Mar. 2020, doi: 10.1109/TVT.2020.2967124.

[16] A. Shamsoshoara, F. Afghah, A. Razi, S. Mousavi, J. Ashdown, and K. Turk, "An autonomous spectrum management scheme for unmanned aerial vehicle networks in disaster relief operations," *IEEE Access*, vol. 8, pp. 58064–58079, 2020, doi: 10.1109/ACCESS.2020.2982932.

[17] S. Hosseinalipour, A. Rahmati, D. Y. Eun, and H. Dai, "Energy-aware stochastic UAV-assisted surveillance," *IEEE Trans. Wireless Commun.*, vol. 20, no. 5, pp. 2820–2837, May 2021, doi: 10.1109/TWC.2020.3044490.

[18] P. K. R. Maddikunta, S. Hakak, M. Alazab, S. Bhattacharya, T. R. Gadekallu, W. Z. Khan, and Q.-V. Pham, "Unmanned aerial vehicles in smart agriculture: Applications, requirements, and challenges," *IEEE Sensors J.*, vol. 21, no. 16, pp. 17608–17619, Aug. 2021, doi: 10.1109/JSEN.2021.3049471.

[19] S. Seng, G. Yang, X. Li, H. Ji, and C. Luo, "Energy-efficient communications in unmanned aerial relaying systems," *IEEE Trans. Netw. Sci. Eng.*, vol. 8, no. 4, pp. 2780–2791, Dec. 2021, doi: 10.1109/TNSE.2021.3064317.

[20] S. Huang, Z. Zeng, K. Ota, M. Dong, T. Wang, and N. Xiong, "An intelligent collaboration trust interconnections system for mobile information control in ubiquitous 5G networks," *IEEE Trans. Netw. Sci. Eng.*, vol. 8, no. 1, pp. 347–365, Mar. 2020, doi: 10.1109/TNSE.2020.3038454.

[21] W. Miao, C. Luo, G. Min, Y. Mi, and H. Wang, "Unlocking the potential of 5G and beyond networks to support massive access of ground and air devices," *IEEE Trans. Netw. Sci. Eng.*, vol. 8, no. 4, pp. 2825–2836, Oct. 2021, doi: 10.1109/TNSE.2021.3051294.

[22] Y. Xu, G. Zhenguo, and N. Qiang, "Unmanned aerial vehicle-assisted node localization for wireless sensor networks," *Int. J. Distrib. Sensor Netw.*, vol. 13, no. 12, pp. 1–13, Dec. 2017.

[23] M. Atif, R. Ahmad, W. Ahmad, L. Zhao, and J. J. P. C. Rodrigues, "UAV-assisted wireless localization for search and rescue," *IEEE Syst. J.*, vol. 15, no. 3, pp. 3261–3272, Feb. 2021, doi: 10.1109/JSYST.2020.3041573.

[24] T. Liang, T. Zhang, J. Yang, D. Feng, and Q. Zhang, "UAV-aided positioning systems for ground devices: Fundamental limits and algorithms," *IEEE Internet Things J.*, vol. 9, no. 15, pp. 13470–13485, Aug. 2022, doi: 10.1109/JIOT.2022.3144234.

[25] R. Chen, B. Yang, and W. Zhang, "Distributed and collaborative localization for swarming UAVs," *IEEE Internet Things J.*, vol. 8, no. 6, pp. 5062–5074, Mar. 2021, doi: 10.1109/JIOT.2020.3037192.

[26] S. Moon and W. Youn, "A novel movable UWB localization system using UAVs," *IEEE Access*, vol. 10, pp. 41303–41312, 2022, doi: 10.1109/ACCESS.2022.3164701.

[27] Z. Chang, H. Deng, L. You, G. Min, S. Garg, and G. Kaddoum, "Trajectory design and resource allocation for multi-UAV networks: Deep reinforcement learning approaches," *IEEE Trans. Netw. Sci. Eng.*, early access, May 3, 2022, doi: 10.1109/TNSE.2022.3171600.

[28] X. Liu, H. Song, and A. Liu, "Intelligent UAVs trajectory optimization from space-time for data collection in social networks," *IEEE Trans. Netw. Sci. Eng.*, vol. 8, no. 2, pp. 853–864, Apr. 2021, doi: 10.1109/TNSE.2020.3017556.

[29] J. Gribben and A. Boukerche, "Location error estimation in wireless ad hoc networks," *Ad Hoc Netw.*, vol. 13, pp. 504–515, Feb. 2014.

[30] A. Simonetto and G. Leus, "Distributed maximum likelihood sensor network localization," *IEEE Trans. Signal Process.*, vol. 62, no. 6, pp. 1424–1437, Mar. 2014, doi: 10.1109/TSP.2014.2302746.

[31] C. Zhao, Y. Xu, and H. Huang, "Weighted centroid localization based on compressive sensing," Wireless Netw., vol. 20, no. 6, pp. 1527–1540, Jan. 2014.

[32] N. Irfan, M. Bolic, M. C. E. Yagoub, and V. Narasimhan, "Neural-based approach for localization of sensors in indoor environment," Telecommun. Syst., vol. 44, nos. 1–2, pp. 149–158, Jun. 2010.

[33] Z. Guo, Y. Guo, F. Hong, Z. Jin, Y. He, Y. Feng, and Y. Liu, "Perpendicular intersection: Locating wireless sensors with mobile beacon," IEEE Trans. Veh. Technol., vol. 59, no. 7, pp. 3501–3509, Sep. 2010, doi: 10.1109/TVT.2010.2049391.

[34] H. Cui and Y. Wang, "Four-mobile-beacon assisted localization in three-dimensional wireless sensor networks," Comput. Electr. Eng., vol. 38, no. 3, pp. 652–661, May 2012.

[35] G. Han, J. Jiang, C. Zhang, T. Q. Duong, M. Guizani, and G. K. Karagiannidis, "A survey on mobile anchor node assisted localization in wireless sensor networks," IEEE Commun. Surveys Tuts., vol. 18, no. 3, pp. 2220–2243, 3rd Quart., 2016, doi: 10.1109/COMST.2016.2544751.

[36] L. Oliveira, H. Li, L. Almeida, and T. E. Abrudan, "RSSI-based relative localisation for mobile robots," Ad Hoc Netw., vol. 13, pp. 321–335, Feb. 2014.

[37] J. Aspnes, "A theory of network localization," IEEE Trans. Mobile Comput., vol. 5, no. 12, pp. 1663–1678, Dec. 2006, doi: 10.1109/TMC.2006.174.

[38] F. Wen and C. Liang, "Fine-grained indoor localization using single access point with multiple antennas," IEEE Sensors J., vol. 15, no. 3, pp. 1538–1544, Mar. 2015, doi: 10.1109/JSEN.2014.2364121.

[39] P. Tarrío, A. M. Bernardos, and J. R. Casar, "An energy-efficient strategy for accurate distance estimation in wireless sensor networks," Sensors, vol. 12, no. 11, pp. 15438–15466, Nov. 2012.

[40] H. Xiong, Z. Chen, B. Yang, and R. Ni, "TDOA localization algorithm with compensation of clock offset for wireless sensor networks," China Commun., vol. 12, no. 10, pp. 193–201, Oct. 2015, doi: 10.1109/CC.2015.7315070.

[41] Y. Liu, Y. H. Hu, and Q. Pan, "Distributed, robust acoustic source localization in a wireless sensor network," IEEE Trans. Signal Process., vol. 60, no. 8, pp. 4350–4359, Aug. 2012, doi: 10.1109/TSP.2012.2199314.

[42] Y. Xu, J. Zhou, and P. Zhang, "RSS-based source localization when path-loss model parameters are unknown," IEEE Commun. Lett., vol. 18, no. 6, pp. 1055–1058, Jun. 2014, doi: 10.1109/LCOMM.2014.2318031.

[43] T. Qiao, Y. Zhang, and H. Liu, "Nonlinear expectation maximization estimator for TDOA localization," IEEE Wireless Commun. Lett., vol. 3, no. 6, pp. 637–640, Dec. 2014, doi: 10.1109/LWC.2014.2364023.

[44] N. Bulusu, J. Heidemann, and D. Estrin, "GPS-less low-cost outdoor localization for very small devices," IEEE Pers. Commun., vol. 7, no. 5, pp. 28–34, Oct. 2000, doi: 10.1109/98.878533.

[45] L. Gui, F. Xiao, Y. Zhou, F. Shu, and T. Val, "Connectivity based DV-hop localization for Internet of Things," IEEE Trans. Veh. Technol., vol. 69, no. 8, pp. 8949–8958, Aug. 2020, doi: 10.1109/TVT.2020.2998093.

[46] M. Singh, S. K. Bhoi, and P. M. Khilar, "Geometric constraint-based range-free localization scheme for wireless sensor networks," IEEE Sensors J., vol. 17, no. 16, pp. 5350–5366, Aug. 2017, doi: 10.1109/JSEN.2017.2725343.

[47] L. A. Villas, D. L. Guidoni, G. Maia, R. W. Pazzi, J. Ueyama, and A. A. F. Loureiro, "An energy efficient joint localization and synchronization solution for wireless sensor networks using unmanned aerial vehicle," Wireless Netw., vol. 21, no. 2, pp. 485–498, Feb. 2015.

[48] M. Y. Arafat and S. Moh, "Bio-inspired approaches for energy-efficient localization and clustering in UAV networks for monitoring wildfires in remote areas," IEEE Access, vol. 9, pp. 18649–18669, 2021, doi: 10.1109/ACCESS.2021.3053605.

[49] F. Shahzad, T. R. Sheltami, and E. M. Shakshuki, "Multi-objective optimization for a reliable localization scheme in wireless sensor networks," J. Commun. Netw., vol. 18, no. 5, pp. 796–805, Oct. 2016, doi: 10.1109/JCN.2016.000108.

[50] R. Garg, A. L. Verna, and M. Wu, "An efficient gradient descent approach to secure localization in resource constrained wireless sensor networks," IEEE Trans. Inf. Forensics Security, vol. 7, no. 2, pp. 717–730, Apr. 2012, doi: 10.1109/TIFS.2012.2184094.

[51] J. Lovon-Melgarejo, M. Castillo-Cara, O. Huarcaya-Canal, L. Orozco-Barbosa, and I. Garcia-Varea, "Comparative study of supervised learning and Metaheuristic algorithms for the development of Bluetooth-based indoor localization mechanisms," IEEE Access, vol. 7, pp. 26123–26135, 2019, doi: 10.1109/ACCESS.2019.2899736.

[52] Q. Shi, C. He, H. Chen, and L. Jiang, "Distributed wireless sensor network localization via sequential greedy optimization algorithm," IEEE Trans. Signal Process., vol. 58, no. 6, pp. 3328–3340, Jun. 2010, doi: 10.1109/TSP.2010.2045416.

[53] V. R. Sabbella, D. R. Edla, A. Lipare, and S. R. Parne, "An efficient localization approach in wireless sensor networks using krill herd optimization algorithm," IEEE Syst. J., vol. 15, no. 2, pp. 2432–2442, Jun. 2021, doi: 10.1109/JSYST.2020.3004527.

[54] Y. Wang, "Acoustic localization of partial discharge sources in power transformers using a particle-swarm-optimization-route-searching algorithm," IEEE Trans. Dielectr. Electr. Insul., vol. 24, no. 6, pp. 3647–3656, Dec. 2017, doi: 10.1109/TDEI.2017.006857.

[55] H. Chen, T. Ballal, N. Saeed, M.-S. Alouini, and T. Y. Al-Naffouri, "A joint TDOA-PDOA localization approach using particle swarm optimization," IEEE Wireless Commun. Lett., vol. 9, no. 8, pp. 1240–1244, Aug. 2020, doi: 10.1109/LWC.2020.2986756.

[56] R. Harikrishnan, V. J. S. Kumar, and P. S. Ponmalar, "A comparative analysis of intelligent algorithms for localization in wireless sensor networks," Wireless Pers. Commun., vol. 87, no. 3, pp. 1057–1069, Apr. 2016.

[57] D. Qiao and G. K. Pang, "A modified differential evolution with heuristic algorithm for nonconvex optimization on sensor network localization," IEEE Trans. Veh. Technol., vol. 65, no. 3, pp. 1676–1689, Mar. 2016, doi: 10.1109/TVT.2015.2409319.

[58] A. Akbas, H. U. Yildiz, A. M. Ozbayoglu, and B. Tavli, "Neural network based instant parameter prediction for wireless sensor network optimization models," Wireless Netw., vol. 25, no. 6, pp. 3405–3418, 2019.

[59] S. K. Gharghan, R. Nordin, M. Ismail, and J. A. Ali, "Accurate wireless sensor localization technique based on hybrid PSO-ANN algorithm for indoor and outdoor track cycling," IEEE Sensors J., vol. 16, no. 2, pp. 529–541, Jan. 2016, doi: 10.1109/JSEN.2015.2483745.

[60] S. Kumar, R. Sharma, and E. R. Vans, "Localization for wireless sensor networks: A neural network approach," Int. J. Comput. Netw. Commun., vol. 8, no. 1, pp. 61–71, Jan. 2016.

[61] V. Annepu, A. Rajesh, and K. Bagadi, "Radial basis function-based node localization for unmanned aerial vehicle-assisted 5G wireless sensor networks," Neural Comput. Appl., vol. 33, no. 19, pp. 12333–12346, Mar. 2021.

[62] S. Haykin, Neural Networks. New York, NY, USA: Pearson, 1999, pp. 278–339.

[63] V. Annepu and A. Rajesh, "Implementation of self adaptive mutation factor and cross-over probability based differential evolution algorithm for node localization in wireless sensor networks," Evol. Intell., vol. 12, no. 3, pp. 469–478, May 2019.

[64] V. Annepu and A. Rajesh, "Implementation of an efficient artificial bee colony algorithm for node localization in unmanned aerial vehicle assisted wireless sensor networks," Wireless Pers. Commun., vol. 114, no. 3, pp. 2663–2680, Oct. 2020, doi: 10.1007/s11277-020-07496-8.

[65] V. Annepu and A. Rajesh, "An unmanned aerial vehicle-aided node localization using an efficient multilayer perceptron neural network in wireless sensor networks," Neural Comput. Appl., vol. 32, no. 15, pp. 11651–11663, Dec. 2019.

[66] V. Annepu, A. Rajesh, and K. Bagadi, "Radial basis function-based node localization for unmanned aerial vehicle-assisted 5G wireless sensor networks," Neural Comput. Appl., vol. 33, no. 19, pp. 12333–12346, Mar. 2021, doi: 10.1007/s00521-021-05835-9.

[67] V. Annepu and R. Anbazhagan, "Implementation of an efficient extreme learning machine for node localization in unmanned aerial vehicle assisted wireless sensor networks," Int. J. Commun. Syst., vol. 33, no. 10, Sep. 2019, Art. no. e4173, doi: 10.1002/dac.4173.

[68] R. Storn and K. Price, "Differential evolution—A simple and efficient heuristic for global optimization over continuous spaces," J. Global Optim., vol. 11, no. 4, pp. 341–359, 1997.

[69] K. D. Jong, "Adaptive system design: A genetic approach," IEEE Trans. Syst., Man, Cybern., vol. SMC-10, no. 9, pp. 566–574, Sep. 1980, doi: 10.1109/TSMC.1980.4308561.

[70] J. Brest, S. Greiner, B. Boskovic, M. Mernik, and V. Zumer, "Self-adapting control parameters in differential evolution: A comparative study on numerical benchmark problems," IEEE Trans. Evol. Comput., vol. 10, no. 6, pp. 646–657, Dec. 2006, doi: 10.1109/TEVC.2006.872133.

[71] A. K. Qin, V. L. Huang, and P. N. Suganthan, "Differential evolution algorithm with strategy adaptation for global numerical optimization," IEEE Trans. Evol. Comput., vol. 13, no. 2, pp. 398–417, Apr. 2009, doi: 10.1109/TEVC.2008.927706.

[72] J. Brest and M. S. Maučec, "Self-adaptive differential evolution algorithm using population size reduction and three strategies," *Soft Comput.*, vol. 15, no. 11, pp. 2157–2174, Nov. 2011.

[73] D. Karaboga, "An idea based on honey bee swarm for numerical optimization," Erciyes Univ., Kayseri, Turkey, Tech. Rep. TR06, Oct. 2005.

[74] D. Karaboga and B. Akay, "A comparative study of artificial bee colony algorithm," *Appl. Math. Comput.*, vol. 214, no. 1, pp. 108–132, Aug. 2009.

[75] W. Gao, S. Liu, and L. Huang, "A global best artificial bee colony algorithm for global optimization," *J. Comput. Appl. Math.*, vol. 236, no. 11, pp. 2741–2753, 2012.

[76] D. W. Ruck, S. K. Rogers, M. Kabrisky, M. E. Oxley, and B. W. Suter, "The multilayer perceptron as an approximation to a Bayes optimal discriminant function," *IEEE Trans. Neural Netw.*, vol. 1, no. 4, pp. 296–298, Dec. 1990, doi: 10.1109/72.80266.

[77] Z. H. Michalopoulou, L. W. Nolte, and D. Alexandrou, "Performance evaluation of multilayer perceptrons in signal detection and classification," *IEEE Trans. Neural Netw.*, vol. 6, no. 2, pp. 381–386, Mar. 1995, doi: 10.1109/72.363473.

[78] F. Murtagh, "Multilayer perceptrons for classification and regression," *Neurocomputing*, vol. 2, nos. 5–6, pp. 183–197, Jul. 1991, doi: 10.1016/0925-2312(91)90023-5.

[79] S. Das, "A novel concept of embedding orthogonal basis function expansion block in a neural equalizer structure for digital communication channel," *Neural Comput. Appl.*, vol. 21, no. 3, pp. 481–488, Apr. 2012.

[80] K. P. Bagadi and S. Das, "Neural network-based multiuser detection for SDMA–OFDM system over IEEE 802.11n indoor wireless local area network channel models," *Int. J. Electron.*, vol. 100, no. 10, pp. 1332–1347, Oct. 2013.

[81] K. P. Bagadi and S. Das, "Neural network-based adaptive multiuser detection schemes in SDMA–OFDM system for wireless application," *Neural Comput. Appl.*, vol. 23, nos. 3–4, pp. 1071–1082, Sep. 2013.

[82] K. P. Bagadi, V. Annepu, and S. Das, "Recent trends in multiuser detection techniques for SDMA–OFDM communication system," *Phys. Commun.*, vol. 20, pp. 93–108, Sep. 2016.

[83] C. Ravikumar and K. Bagadi, "MC-CDMA receiver design using recurrent neural networks for eliminating multiple access interference and nonlinear distortion," *Int. J. Commun. Sys.*, vol. 30, pp. 1–13, Nov. 2017.

[84] K. Hornik, M. Stinchcombe, and H. White, "Multilayer feedforward networks are universal approximators," *Neural Netw.*, vol. 2, no. 5, pp. 359–366, Dec. 1989.

[85] D. S. Broomhead and D. Lowe, "Multivariable functional interpolation and adaptive networks," *Complex Syst.*, vol. 2, no. 3, pp. 321–355, Jan. 1988.

[86] J. Moody and C. J. Darken, "Fast learning in networks of locally-tuned processing units," *Neural Comput.*, vol. 1, no. 2, pp. 281–294, 1989, doi: 10.1162/neco.1989.1.2.281.

[87] I. Cha and S. A. Kassam, "Channel equalization using adaptive complex radial basis function networks," *IEEE J. Sel. Areas Commun.*, vol. 13, no. 1, pp. 122–131, Jan. 1995, doi: 10.1109/49.363139.

[88] K. P. Bagadi and S. Das, "Efficient complex radial basis function model for multiuser detection in a space division multiple access/multiple-input multiple-output–orthogonal frequency division multiplexing system," *IET Commun.*, vol. 7, no. 13, pp. 1394–1404, Sep. 2013.

[89] C. V. Ravikumar and K. Bagadi, "Design of MC-CDMA receiver using radial basis function network to mitigate multiple access interference and nonlinear distortion," *Neural Comput. Appl.*, vol. 31, no. S2, pp. 1263–1273, Feb. 2019.

[90] G.-B. Huang, Q.-Y. Zhu, and C.-K. Siew, "Extreme learning machine: Theory and applications," *Neurocomputing*, vol. 70, nos. 1–3, pp. 489–501, 2006.

[91] G.-B. Huang, D. H. Wang, and Y. Lan, "Extreme learning machines: A survey," *Int. J. Mach. Learn. Cybern.*, vol. 2, no. 2, pp. 107–122, Jun. 2011.

[92] R. Minhas, A. Baradarani, S. Seifzadeh, and Q. M. J. Wu, "Human action recognition using extreme learning machine based on visual vocabularies," *Neurocomputing*, vol. 73, nos. 10–12, pp. 1906–1917, 2010.

[93] G. B. Huang, H. Zhou, X. Ding, and R. Zhang, "Extreme learning machine for regression and multiclass classification," *IEEE Trans. Syst., Man, Cybern. B, Cybern.*, vol. 42, no. 2, pp. 513–529, Feb. 2012, doi: 10.1109/TSMCB.2011.2168604.

[94] C. Pan, D. S. Park, Y. Yang, and H. M. Yoo, "Leukocyte image segmentation by visual attention and extreme learning machine," *Neural Comput. Appl.*, vol. 21, no. 6, pp. 1217–1227, 2012.

VISALAKSHI ANNEPU received the B.Tech. degree in computer science and engineering from Jawaharlal Nehru Technical University, Kakinada, India, in 2011, the M.Tech. degree in computer science and Technology from Andhra University, Visakhapatnam, India, in 2013, and the Ph.D. degree in computer networks from the VIT Vellore, India, in 2020. She worked as an Assistant Professor with the Department of Computer Engineering, Sri Sivani Institute of Technology, Srikakulam, Andhra Pradesh, during June 2014–May 2016. Her research interests include wireless networking, artificial intelligence, soft computing techniques, and neural networks.

DEEPIKA RANI SONA is currently a Senior Faculty with the School of Electronics Engineering, VIT University. She has experience of research and development in the field of mobile opportunistic networks, device-to-device communications, network virtualization, energy-efficient wireless networks, future internet, the IoT, 5G, and machine learning. She worked on an automated car parking project at VIT University. She has extensive experience of supervising B.Tech. and M.Tech. students/projects in D2D, the IoT, ML, robotics, and image processing.

CHINTHAGINJALA V. RAVIKUMAR received the M.Tech. degree in digital electronics and communication system from Jawaharlal Nehru Technology University, Anantapur, in 2009, and the Ph.D. degree in communication networks from the VIT Vellore, India, in 2018. He currently works as an Assistant Professor SG at the Institute of Vellore Institute of Technology, School of Electronics Engineering, Department of Embedded Technology. His current research interests include communication networks, machine learning, deep learning, wireless sensor networks, and information security.

KALAPRAVEEN BAGADI received the B.E. degree in electronics and communication engineering from Andhra University, India, in 2006, the M.Tech. degree in electronic systems and communication from the National Institute Technology, Rourkela, India, in 2009, and the Ph.D. degree in wireless communication from the Department of Electrical Engineering, National Institute of Technology, Rourkela. He is currently working as an Associate Professor Senior with the School of Electronics Engineering (SENSE), VIT Vellore, India. He has published several research articles in various journals. He has finished six Ph.D. thesis and also guiding two Ph.D. scholars. He has published over 50 research papers in refereed international journals and conferences. His work has been cited more than 500 times at Google Scholar. His research interests include SDMA, MIMO, OFDM, wireless communications, and artificial intelligence. He is also a Reviewer of the journals like *Wireless Personal Communications*, *IET Communications*, and *Telecommunication Systems*.

MOHAMMAD ALIBAKHSHIKENARI (Member, IEEE) was born in Mazandaran, Iran, in February 1988. He received the Ph.D. degree (Hons.) with European Label in electronics engineering from the University of Rome "Tor Vergata," Italy, in February 2020. He was a Ph.D. Visiting Researcher at the Chalmers University of Technology, Sweden, in 2018. His training during the Ph.D. included a research stage with Swedish company Gap Waves AB. He is currently with the Department of Signal Theory and Communications, Universidad Carlos III de Madrid (uc3m), Spain, as the Principal Investigator of the CONEX-Plus Talent Training Program and Marie Sklodowska-Curie Actions. He is also a Lecturer with the Electromagnetic Fields and Electromagnetic Laboratory, Department of Signal Theory and Communications. His research interests include electromagnetic systems, antennas and wave-propagations, metamaterials and metasurfaces, synthetic aperture radars (SAR), multiple-input multiple-output (MIMO) systems, RFID tag antennas, substrate integrated waveguides (SIWs), impedance matching circuits, microwave components, millimeter-waves and terahertz integrated circuits, gap waveguide technology, beamforming matrix, and reconfigurable intelligent surfaces (RIS). The above research lines have produced more than 200 publications on international journals, presentations within international conferences, and book chapters with a total number of the citations more than 3300 and H-index of 40 reported by Google Scholar. He was a recipient of the three years research grant funded by the Universidad Carlos III de Madrid and the European Union's Horizon 2020 Research and Innovation Program under the Marie Sklodowska-Curie Grant in July 2021, the two years research grant funded by the University of Rome "Tor Vergata" started in November 2019, the three years Ph.D. Scholarship funded by the University of Rome "Tor Vergata" started in November 2016, and the two Young Engineer Awards of the 47th and 48th European Microwave Conference held in Nuremberg, Germany, in 2017, and in Madrid, Spain, in 2018, respectively. For academic year 2021–2022, he received the "Teaching Excellent Acknowledgement" Certificate for the course of electromagnetic fields from Vice-Rector of studies of uc3m. His research article entitled "High-Gain Metasurface in Polyimide On-Chip Antenna Based on CRLH-TL for Sub Terahertz Integrated Circuits" published in Scientific Reports was awarded as the Best Month Paper at the University of Bradford, U.K., in April 2020. He is serving as an Associate Editor for *Radio Science* and *The Journal of Engineering* (IET). He also acts as a referee in several highly reputed journals and international conferences.

AYMAN A. ALTHUWAYB (Member, IEEE) received the B.Sc. degree (Hons.) in electrical engineering (electronics and communications) from Jouf University, Saudi Arabia, the M.Sc. degree in electrical engineering from California State University, Fullerton, CA, USA, in 2015, and the Ph.D. degree in electrical engineering from Southern Methodist University, Dallas, TX, USA, in 2018. He is currently an Assistant Professor with the Department of Electrical Engineering, Jouf University. His current research interests include antenna design and propagation, microwaves and millimeter-waves, wireless power transfer, ultra-wideband and multiband antenna, filters, and others.

BADER ALALI received the B.Sc. degree (Hons.) in electrical engineering from Jouf University, Saudi Arabia, in 2011, and the M.Sc. degree in electrical engineering from California State University, Fullerton, CA, USA, in 2015. He is currently pursuing the Ph.D. degree with the Institute of Electronic, Communications and Information Technology, Queen's University Belfast, Belfast, U.K. He is also a Lecturer at the Department of Electrical Engineering, Jouf University. His current research interests include millimeter-wave and microwave components and circuits, lens antennas, reflectarray antennas, and electromagnetic field theory.

BAL S. VIRDEE (Senior Member, IEEE) received the B.Sc. and M.Phil. degrees in communications engineering from the University of Leeds, U.K., and the Ph.D. degree in electronic engineering from the University of London, U.K. He worked in industry for various companies, including Philips, U.K., as an Research and Development Engineer with Filtronic Components Ltd.., as a Future Products Developer in the area of RF/microwave communications. He has taught at several academic institutions before joining London Metropolitan University, where he is currently a Professor of microwave communications with the Faculty of Life Sciences and Computing, where he heads the Center for Communications Technology and the Director of London Metropolitan Microwaves. His research, in collaboration with industry and academia, is in the area of microwave wireless communications encompassing mobile phones to satellite technology. He has chaired technical sessions at IEEE international conferences and published numerous research papers. He is an Executive Member of IET's Technical and Professional Network Committee on RF/Microwave Technology. He is a fellow of IET.
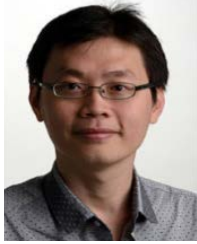
GIOVANNI PAU (Member, IEEE) received the bachelor's degree in telematic engineering from the University of Catania, Italy, and the master's (cum Laude) and Ph.D. degrees in telematic engineering from Kore University of Enna, Italy. He is currently an Associate Professor at the Faculty of Engineering and Architecture, Kore University of Enna. He is the author/coauthor of more than 80 refereed papers published in journals and conference proceedings. His research interests include wireless sensor networks, fuzzy logic controllers, intelligent transportation systems, the Internet of Things, smart homes, and network security. He has been involved in several international conferences as a session co-chair and a technical program committee member. He serves/served as a leading guest editor in special issues of several international journals. He is an Editorial Board Member and an Associate Editor of several journals, such as IEEE Access, *Wireless Networks* (Springer), *EURASIP Journal on Wireless Communications and Networking* (Springer), *Wireless Communications and Mobile Computing* (Hindawi), *Sensors* (MDPI), and *Future Internet* (MDPI), to name a few.

IYAD DAYOUB (Senior Member, IEEE) received the B.Eng. degree in telecommunications and electronics in Syria, in 1993, the M.A.Sc. degree in electrical engineering from the National Polytechnic Institute of Lorraine (INPL), and the Ph.D. degree from the University of Valenciennes and the Institute of Electronics, Microelectronics and Nanotechnology (IEMN), in 2001. He worked as a System Engineer with Siemens, Middle East; and a Researcher with Alcatel Business Systems, Alcatel, Colombes, Paris. He was an Adjunct Professor with Concordia University, Montreal, from 2010 to 2014. He is currently a Professor of communications engineering. His current research activities at IEMN, Université Polytechnique Hauts-de-France (UPHF) and INSA H-d-F are focused on wireless communications, high-speed communications, cognitive radio, and hybrid radio-optic technologies. He was a member of the National Council of Universities (CNU), France, from 2007 to 2014, in the area of electrical engineering, electronics, photonics, and systems. He is a member of several international conference advisory committees, technical program committees, and organization committees, such as VTC, GLOBECOM, ICC, PIMRC, and WWC.

CHAN HWANG SEE (Senior Member, IEEE) received the B.Eng. (Hons.) and Ph.D. degrees in electronic, telecommunication and computer engineering from the University of Bradford, U.K., in 2002 and 2007, respectively. He is currently an Associate Professor with the School of Computing, Engineering and the Built Environment, Edinburgh Napier University, U.K. Previously, he was the Head of Electrical Engineering and Mathematics. Prior to this, he was a Senior Lecturer (Program Leader) in electrical and electronic engineering with the School of Engineering, University of Bolton, U.K. Before this, he was a Senior Research Fellow with the Antennas and Applied Electromagnetics Research Group, University of Bradford. He has published over 130 peer-reviewed journal articles in these research areas. He is the coauthor of one book and three book chapters. His research interests include wireless sensor network system design, computational electromagnetism, antennas, microwave circuits, wireless power transfer, and acoustic sensor design. He is a fellow of the Institution of Engineering and Technology. He is also a fellow of the Higher Education Academy and a Full Member of the EPSRC Review College. He was a recipient of two Young Scientist Awards from the International Union of Radio Science (URSI) and Asia-Pacific Radio Science Conference (AP-RASC), in 2008 and 2010, respectively. He was awarded the Certificate of Excellence for his successful Knowledge Transfer Partnership (KTP) with Yorkshire Water on the design and implementation of a wireless sensor system for sewerage infrastructure monitoring, in 2009. He is a Chartered Engineer. He is an Associate Editor of IEEE Access and an Editor of the *Journal of Electronics and Electrical Engineering*, *Scientific Reports*, *Computer Science* (PeerJ), *PLOS One*, and *Wireless Power Transfer* journals.

FRANCISCO FALCONE (Senior Member, IEEE) received the degree in telecommunication engineering and the Ph.D. degree in communication engineering from the Universidad Pública de Navarra (UPNA), Spain, in 1999 and 2005, respectively. From 1999 to 2000, he was a Microwave Network Engineer with Siemens-Italtel, Málaga. From 2000 to 2008, he was a Mobile Access Network Engineer with Telefónica Móviles, Pamplona. In 2009, he co-founded Tafco Metawireless, spin-off of the UPNA (with EIBT national label), of which he was its first manager. In parallel, from 2003 to 2009, he was an Assistant Lecturer with the Department of Electrical and Electronic Engineering, UPNA. In June 2009, he became an Associate Professor and since September 2022, he has been a Full Professor at the EEC Department, UPNA. From 2011 to 2012, he was the Secretary of the Department of Electrical, Electronic and Communication Engineering, UPNA. From January 2012 to July 2018 and from July 2019 to November 2021, he was the Head of the Department of Electrical, Electronic and Communication Engineering, UPNA. In 2018, he was a Visiting Professor at the Kuwait College of Science and Technology, Kuwait, for three months. He is also affiliated with the Smart Cities Institute, Public University of Navarra, a multidisciplinary research institute with over 100 researchers, being Head of the Institute, since May 2021, working on contextual and interactive environments solutions, through the integration of heterogeneous wireless communications networks, based on HetNet and the IoT. Since June 2022, he has been a Distinguished Visiting Professor of telecommunications with the School of Engineering and Science, Tecnologico de Monterrey, Mexico. He has over 600 contributions in indexed international journals, book chapters, and conference contributions. His research interests include computational electromagnetics applied to the analysis of complex electromagnetic scenarios, with a focus on the analysis, design, and implementation of heterogeneous wireless networks to enable context-aware environments. He has been awarded several research awards: CST Best Paper Award 2003 and 2005, Prize of the Official Association of Telecommunications Engineers 2005 for the Best Doctoral Thesis, UPNA Ph.D. Award 2004–2006 in Experimental Sciences, 1st Prize Juan López de Peñalver 2010 to the Best Young Researcher, Real Academia de Ingeniería de España, XII Talgo Foundation Award for Technological Innovation with the proposal "Implementation of an Environment for the Railway Ecosystem," ECSA-2 Best Paper Award in 2015, Best Paper Award IISA, in 2015, ECSA Award-3 Best Paper Award, in 2016, ECSA-4 Best Paper Award, in 2018, Best Paper Award ISSI, in 2019, and the IIoT 2020 Best Paper Award.

● ● ●